J Physiol 592.9 (2014) pp 2013–2033

The Journal of Physiology

Short-term sustained hypoxia induces changes in the coupling of sympathetic and respiratory activities in rats

Davi J. A. Moraes, Leni G. H. Bonagamba, Kauê M. Costa, João H. Costa-Silva, Daniel B. Zoccal and Benedito H. Machado

Department of Physiology, School of Medicine of Ribeirão Preto, University of São Paulo, Ribeirão Preto, Brazil

Key points

- Hypoxia activates peripheral chemoreceptors producing an increase in breathing and arterial pressure.
- In conditions of sustained hypoxia, an increase in ventilation and arterial blood pressure is observed that persists after the return to normoxia.
- We show in rats that sustained hypoxia for 24 h produces glutamate-dependent changes in the activity of expiratory and sympathetic neurones of the rostral ventrolateral medulla, which are essential for the control of respiratory and sympathetic activities.
- These neuronal changes induced by sustained hypoxia are critical for the emergence of coupled active expiration and augmented sympathetic activity.
- These findings contribute to a better understanding of cardiorespiratory adjustments associated with sustained hypoxia in individuals experiencing high altitudes.

Abstract Individuals experiencing sustained hypoxia (SH) exhibit adjustments in the respiratory and autonomic functions by neural mechanisms not yet elucidated. In the present study we evaluated the central mechanisms underpinning the SH-induced changes in the respiratory pattern and their impact on the sympathetic outflow. Using a decerebrated arterially perfused *in situ* preparation, we verified that juvenile rats exposed to SH (10% O_2) for 24 h presented an active expiratory pattern, with increased abdominal, hypoglossal and vagal activities during late-expiration (late-E). SH also enhanced the activity of augmenting-expiratory neurones and depressed the activity of post-inspiratory neurones of the Bötzinger complex (BötC) by mechanisms not related to changes in their intrinsic electrophysiological properties. SH rats exhibited high thoracic sympathetic activity and arterial pressure levels associated with an augmented firing frequency of pre-sympathetic neurones of the rostral ventrolateral medulla (RVLM) during the late-E phase. The antagonism of ionotropic glutamatergic receptors in the BötC/RVLM abolished the late-E bursts in expiratory and sympathetic outputs of SH rats, indicating that glutamatergic inputs to the BötC/RVLM are essential for the changes in the expiratory and sympathetic coupling observed in SH rats. We also observed that the usually silent late-E neurones of the retrotrapezoid nucleus/parafacial respiratory group became active in SH rats, suggesting that this neuronal population may provide the excitatory drive essential to the emergence of active expiration and sympathetic overactivity. We conclude that short-term SH induces the activation of medullary expiratory neurones, which affects the pattern of expiratory motor activity and its coupling with sympathetic activity.

D. B. Zoccal and B. H. Machado are joint last authors.

DOI: 10.1113/jphysiol.2013.262212

(Received 16 July 2013; accepted after revision 3 March 2014; first published online 10 March 2014)
Corresponding author B. H. Machado: Department of Physiology, School of Medicine of Ribeirão Preto, University of São Paulo, 14049-900, Ribeirão Preto, SP, Brazil. Email: bhmachad@fmrp.usp.br

Abbreviations AbN, abdominal nerve; aug-E, augmenting-expiratory; BötC, Bötzinger complex; CIH, chronic intermittent hypoxia; cVN, cervical vagus nerve; E2, expiratory phase 2; HF, high frequency; HN, hypoglossal nerve; HR, heart rate; late-E, late-expiration; LF, low frequency; MAP, mean arterial pressure; pFRG, parafacial respiratory group; PN, phrenic nerve; post-I, post-inspiratory; pre-I, pre-inspiratory; RTN, retrotrapezoid nucleus; RVLM, rostral ventrolateral medulla; SAP, systolic arterial pressure; SGP, subglottal pressure; SH, sustained hypoxia; tSN, thoracic sympathetic nerve; VRC, ventral respiratory column.

Introduction

Respiratory and autonomic functions are precisely controlled by complex neural networks in order to optimize blood gas exchange/perfusion and maintain homeostasis (Gilbey, 2007; Zoccal *et al.* 2009*b*; Ben-Tal *et al.* 2012). The pattern and strength of respiratory and autonomic coupling may change and generate appropriate cardiorespiratory responses to metabolic challenges (Dick *et al.* 2004; Molkov *et al.* 2011). Such respiratory and autonomic reflex adjustments are observed in conditions of hypoxia (Dick *et al.* 2004; Mandel & Schreihofer, 2009; Costa-Silva *et al.* 2010) and are triggered by the activation of peripheral chemosensitive cells located in the carotid bodies (Barros *et al.* 2002; Lahiri *et al.* 2006). Excitatory inputs from the peripheral chemoreceptors activate neural pathways in the brainstem to increase minute ventilation (Powell *et al.* 1998; Teppema & Dahan, 2010) by changes in the inspiratory and expiratory motor activities (Braga *et al.* 2007; Moraes *et al.* 2012*a*). In conjunction with the respiratory responses, peripheral chemoreflex activation also produces a marked increase in sympathetic nerve activity to elevate arterial pressure (Braga *et al.* 2007). In conditions of acute hypoxia (seconds to minutes), the activation of the respiratory motor and sympathetic activities is transitory and returns to baseline when the arterial partial pressure of oxygen is back to the normal level.

Long periods of sustained hypoxia (SH; hours or days), such as observed at high altitudes, lead to important plastic changes in the mechanisms controlling cardiorespiratory functions (Forster *et al.* 1971; Powell *et al.* 1998; Rostrup, 1998). There is evidence that SH induces a time-dependent increase in baseline ventilation, named ventilatory acclimatization to hypoxia (Powell *et al.* 1998). This acclimatization in rats is characterized by an increase in tidal volume (Aaron & Powell, 1993) probably due to changes in oxygen sensitivity of the carotid bodies (Kääb *et al.* 2005; Powell, 2007) as well as changes in the brainstem neuronal network involved with the respiratory response to peripheral chemoreflex activation (Powell *et al.* 2000; Zhang *et al.* 2009). However, the patterns of inspiratory and expiratory cranial and motor outputs associated with the ventilatory acclimatization to SH remain unclear. Moreover, it is important to explore a possible correlation between the ventilatory responses to SH and the alterations in the activity of respiratory neurones located in the ventral surface of medulla, which are essential for respiratory rhythm and pattern generation (Richter, 1982; Smith *et al.* 1991; Janczewski & Feldman, 2006; Smith *et al.* 2007; Molkov *et al.* 2010).

In relation to the cardiovascular function, the effects of SH on baseline sympathetic nerve activity are not completely understood (Rostrup, 1998; Hainsworth & Drinkhill, 2007). Healthy humans exposed to SH present an increase in muscle sympathetic nerve activity and arterial pressure simultaneously with the development of ventilatory acclimatization to hypoxia (Calbet, 2003; Hansen & Sander, 2003). On the other hand, there is evidence that SH in humans may not modify the levels of muscle sympathetic nerve activity, regardless of the presence of ventilatory response (Tamisier *et al.* 2007). In order to evaluate the consequences of SH on the control of sympathetic activity and arterial pressure, and its possible relationship with the ventilatory response, experiments with animal models are required. These new series of experimental protocols should involve direct measurements of the activity of sympathetic nerves as well as of pre-sympathetic neurones in the rostral ventrolateral medulla, which correspond to the major source of excitatory inputs to sympathetic pre-ganglionic neurones of the spinal cord (Ross *et al.* 1984).

The present study was designed to evaluate the cardiorespiratory changes induced by SH. To reach this goal, we characterized the respiratory and sympathetic motor alterations in rats submitted to short-term SH (24 h) and sought for possible changes in the neuronal networks in the ventral medulla. In addition, we assessed the pattern of phrenic, hypoglossal, vagal and abdominal nerve activities as well as the respiratory medullary neuronal activity in rats submitted to SH. The levels of sympathetic nerve discharge, the respiratory–sympathetic coupling, the activity of pre-sympathetic neurones of the rostral ventrolateral medulla and baseline arterial pressure of SH rats were also evaluated.

Methods

Animals and ethical approval

The experiments were performed on juvenile male Wistar rats (80–120 g) obtained from the Animal Care Unit of the University of São Paulo, Ribeirão Preto, Brazil. All the experimental protocols were approved by the Ethical Committee on Animal Experimentation of the School of Medicine of Ribeirão Preto, University of São Paulo (protocols 019/2006 and 064/2010).

Sustained hypoxia (SH)

The animals were divided into two experimental groups: rats exposed to SH for 24 h and rats maintained under normoxia (control) for the same period of time. Both SH and control rats were housed in collective cages placed inside Plexiglas chambers equipped with gas injectors and sensors for O_2, CO_2, humidity and temperature. The animals were maintained in standard environmental conditions (23 ± 2°C; 12 h/12 h dark/light cycle) with water and chow *ad libitum*. In the SH group, pure N_2 was injected into the chambers to reduce the fraction of inspired O_2 (F_{IO_2}) from 21% to 10%, and this level was maintained for 24 h. In a similar chamber in the same room, the control group was exposed to the F_{IO_2} of 21% and maintained at this level by frequent injections of O_2. The injections of N_2 and O_2 (White Martins, Sertãozinho, Brazil) into the chambers were regulated by a solenoid valve system whose opening–closing control was operated by a computerized system (Oxycycler, Biospherix, Lacona, NY, USA). In both SH and control chambers, the gas injections were performed at the upper level of the chamber to avoid direct gas jets on the animals and unnecessary stress. In distinct SH and control groups, the rats were removed from the chambers at the end of SH and normoxic protocols and maintained for an additional 24 h in normoxia in order to evaluate the reversibility of the cardiovascular and respiratory changes produced by SH.

Procedures in the decerebrated arterially perfused *in situ* preparations

Surgery and perfusion. Immediately after SH or normoxia protocols, the rats were prepared for the *in situ* working heart–brainstem preparations, as previously described (Paton, 1996; Zoccal *et al.* 2008; Moraes *et al.* 2012*a*, 2013). Briefly, the animals were deeply anaesthetized with halothane (AstraZeneca do Brasil Ltda, Cotia, SP, Brazil), transected caudal to the diaphragm, exsanguinated and submerged in a cooled Ringer solution (in mM: NaCl, 125; $NaHCO_3$, 24; KCl, 3; $CaCl_2$, 2.5; $MgSO_4$, 1.25; KH_2PO_4, 1.25; dextrose, 10). They were then decerebrated at the precollicular level and skinned. The descending aorta was isolated and the lungs removed. To expose the ventral medullary surface for microinjections and neuronal recordings, the preparations were placed supine and the brainstem was similarly positioned in all experiments. The trachea, oesophagus, all muscles and connective tissues covering the basilar surface of the occipital bone were removed. The basilar portion of the atlanto-occipital membrane was cut and the bone was removed carefully using a micro-Rongeur (D.L. Micof, São Paulo, Brazil) to expose the ventral surface of the medulla in the antero-posterior extension from the vertebral arteries to the pontine nuclei. Preparations were then transferred to a recording chamber and the descending aorta was cannulated with a double-lumen cannula and retrogradely perfused with Ringer solution containing an oncotic agent (1.25% polyethylene glycol; Sigma, St Louis, MO, USA) and a neuromuscular blocker (vecuronium bromide, 3–4 μg ml^{-1}, Cristália Produtos Químicos Farmacêuticos Ltda, São Paulo, Brazil) using a peristaltic pump (Watson-Marlow 502 S, Falmouth, Cornwall, UK). The perfusion pressure was maintained by adjusting the flow between 21 and 25 ml min^{-1} and by adding vasopressin (0.6–1.2 nM, Sigma) to the perfusate, which was continuously gassed with 5% CO_2 and 95% O_2 (White Martins), warmed to 31–32°C and filtered using a nylon mesh (pore size: 25 μm, Millipore, Billerica, MA, USA).

Nerve recordings and analyses. Sympathetic and respiratory motor nerves were isolated and recorded using bipolar glass suction electrodes held in micromanipulators (Narishige, Tokyo, Japan). Phrenic nerve activity (PN) was recorded from its central end and its rhythmic ramping activity provided a continuous physiological index of preparation viability (Paton, 1996). The cervical vagus (cVN) and hypoglossal (HN) nerves were isolated, cut distally and their central activities recorded. The activity of the thoracic sympathetic nerve (tSN) was recorded from the sympathetic chain at the level of T8–T12. The abdominal nerve (AbN) was isolated from the abdominal muscles at thoracic–lumbar level, cut distally and its activity recorded. All signals recorded were amplified, band-pass filtered (0.5–5 kHz) and acquired with an A/D converter (CED 1401, Cambridge Electronic Design (CED), Cambridge, UK) to a computer using Spike 2 software (CED). All nerves were recorded in absolute units (μV) and analyses were performed off-line in rectified and smoothed (50 ms) signals using Spike 2 software with custom-written scripts. Baseline PN activity was assessed by burst frequency (Hz) and duration (s, time of inspiration). In addition, the time intervals between consecutive PN bursts (time of expiration, s) were also measured. To perform comparisons of the cVN, HN, AbN and tSN recordings between control and SH groups, the changes in the activity of each nerve were expressed as percentage changes in accordance with a scale (0–100%) determined for each preparation, as

previously described (Zoccal *et al.* 2008; Costa-Silva *et al.* 2010; Moraes *et al.* 2012*a*,*c*). In all nerve recordings, the electrical noise (0%) obtained at the end of each experiment after the death of the preparation was subtracted. Phrenic-triggered averages of AbN, cVN, HN and tSN were generated from 1–2 min epochs and divided into three parts: inspiration (coincident with inspiratory PN discharge), post-inspiration (first half of expiratory phase) and expiratory phase 2 (E2; second half of expiratory phase). The AbN, cVN, HN and tSN activities during each respiratory phase were assessed by the measurement of individual area under the curve and normalized by the total area (100%), i.e. sum of areas obtained in inspiratory, post-I and E2. With this approach, we minimized the variability that may occur in multi-fibre recordings. In addition, the duration (s) of the pre-inspiratory component of cVN and HN, preceding the PN burst, was quantified. These analyses were applied for each preparation and data obtained were pooled together and compared between control and SH groups.

Neuronal recordings and analyses. Extra- and intracellular recordings of medullary respiratory and pre-sympathetic neurones were performed in control and SH rats. For extracellular single-unit recordings (Axopatch-200B integrating amplifier; Axon Instruments, Union City, CA, USA) glass microelectrodes (10–30 MΩ) filled with NaCl (3 M) were used. For intracellular recordings, neurones were impaled and stable intracellular recordings were performed to study the effects of SH exposure on membrane potential trajectories and intrinsic electrophysiological properties after fast synaptic transmission blockade (glutamatergic receptors were blocked with 2.5–6.0 mM kynurenic acid, and $GABA_A$ and glycine receptors were blocked by 20 μM bicuculline (free-base) and 1 μM strychnine, respectively). In some experiments the microelectrodes were also filled with methylene blue dye (2%), in 0.5 M sodium acetate, to mark the recording sites by iontophoretic deposition of the dye (10 μA, during 10 min). The microelectrodes were mounted in a 3–D manipulator (Narishige, Tokyo, Japan) and positioned toward the ventral surface of medulla under visual control (binocular microscope; Zeiss, Germany) using surface landmarks (trapezoid body, rootlets of the HN and basilar artery) as anatomical references. All the signals recorded were low-pass filtered (2 kHz) and digitalized (10 kHz) (CED 1401, CED) to a computer using Spike 2 software (CED).

The activities of the following neurones were recorded: (i) post-inspiratory (post-I) and augmenting-expiratory (aug-E) neurones of the Bötzinger complex (BötC); (ii) pre-sympathetic neurones of the rostral ventrolateral medulla (RVLM); and (iii) late-expiratory (late-E) neurones of the retrotrapezoid nucleus/parafacial respiratory group (RTN/pFRG). All these neurones were recorded as previously described (Moraes *et al.* 2012*a*,*c*, 2013). Briefly, expiratory BötC and pre-sympathetic RVLM intracellular recordings were performed at 350–500 μm beneath the ventral surface, 800–1100 μm caudal to the caudal end of the trapezoid body and 1500–1700 μm lateral to the midline (aligned with the rootlets of the HN). Post-I and aug-E neurones were identified by their typical pattern of activity (Smith *et al.* 2007) and the absence of antidromic response to stimulation of the ipsi- or contralateral cVN (0.2 ms, 1 V). The pre-sympathetic neurones were characterized by their inhibitory response to baroreflex activation (electrical stimulation of aortic depressor nerve; 0.2 ms, 3 pulses at 400 Hz) and the presence of antidromic responses to stimulation of spinal segment T8–T12 (0.2 ms). Antidromic responses were distinguished from synaptic excitation by using near threshold stimulation. At this intensity, synaptic events (spontaneous excitatory postsynaptic potential preceding evoked spikes) were absent. Regarding RTN/pFRG neuronal recordings, electrodes for extracellular recordings were positioned 50–100 μm beneath the ventral surface, 500 μm caudal to the caudal end of the trapezoid body, and 1700–2000 μm lateral from the midline. Within this region, late-E neurones were identified as those that were silent in normocapnia but exhibited an increasing pattern of discharge during the late part of the E2 phase when the preparation was exposed to hypercapnia (7–10% CO_2 in the perfusate, GF3/MP Gas Mixing Flow Meter; Cameron Instruments, Port Aransas, TX, USA).

Intracellular recordings of BötC and RVLM neurones were analysed off-line (Clampfit 10; Molecular Devices, Sunnyvalley, CA, USA) in order to measure resting membrane potential, input resistance and repetitive discharge characteristics of the neurones. Input resistance was determined through linear regression applied to the linear portion of the steady-state current–voltage (*I*–*V*) relationship. From recordings of late-E extracellular neuronal activity, window discriminators were used to obtain standard pulses corresponding to the onset of PN discharge and these pulses were used to generate phrenic-triggered histograms of RTN/pFRG late-E unit discharges (bin size 85 ms).

Evaluation of subglottal pressure. Changes in the upper airway resistance were evaluated by direct measurements of subglottal pressure (SGP). The trachea below the larynx was cannulated in the direction of the pharynx with a T-shaped catheter. A constant flow of warmed (31°C) humidified carbogen gas (95% O_2 and 5% CO_2) was injected into one arm of this catheter in the expiratory direction. SGP was recorded in the other side of the T-shaped catheter using a pressure transducer (Model PT 300; Grass, West Warwick, RI, USA). Increases and decreases in SGP were used as indicative of constriction (adduction) and dilatation (abduction), respectively.

These recordings provide an index of the dynamic changes in upper airway resistance every respiratory cycle (Paton & Nolan, 2000).

Microinjections in the ventral surface of medulla. Microinjections of kynurenic acid (200 mM, Sigma-Aldrich, St Louis, MO, USA), an antagonist of glutamatergic ionotropic receptors, were performed bilaterally in the BötC/RVLM, as previously described (Moraes *et al.* 2012*c*). The coordinates used for microinjections were determined in accordance with the location of respiratory and pre-sympathetic neurones in the ventral medulla, as described above. Microinjections were performed using glass micropipettes and the injected volume was approximately 20 nl (Picospritzer II; Parker Instruments, Cleveland, OH, USA).

Histology. At the end of the experiments involving microinjections into the BötC/RVLM, the brainstems of SH preparations were rapidly removed, stored in buffered formalin for 7 days and then serial transverse sections (30 μm thickness) were cut and stained with neutral red using the Nissl method. The sites of microinjections were confirmed by the verification of the tracks of pipettes in the brain tissue. Only the rats in which the tips of the pipettes were centred in the BötC/RVLM were considered for data analysis. In the experiments involving neuronal recordings, the methylene blue dye applied through the recording pipette was visualized in non-stained sections and the centre of the dye application was drawn on an outline of a medulla coronal section.

Procedures in unanaesthetized animals

Measurements of arterial pressure and heart rate. One day before the experimental protocol of SH or normoxia, rats were anaesthetized with tribromoethanol (250 mg kg^{-1}, I.P.; Aldrich, Milwaukee, WI, USA) and a catheter was inserted into the abdominal aorta through the femoral artery (PE–10 connected to PE–50 tubing: Clay Adams, Parsippany, NJ, USA) for arterial pressure measurement. The catheter was tunnelled subcutaneously and exteriorized in the back of the neck. The rats were then housed singly and their respiratory movements were monitored until they regained consciousness. One day after the surgery, the rats were separated in groups for SH or normoxia protocols. After 24 h of SH or normoxia protocols, the rats were moved to the recording room (at normoxic conditions) and a 30 min period was allowed for their adaptation to the new environment. Then, the arterial catheter was connected to a pressure transducer (MLT0380; ADInstruments, Bella Vista, NSW, Australia) and, in turn, to an amplifier (Bridge Amp, ML221; ADInstruments). The pulsatile arterial pressure signals were acquired by a data acquisition system (PowerLab 4/25, ML845, ADInstruments) and recorded on a computer (sampling rate of 2 kHz) using an appropriate software (Chart Pro, ADInstruments). The values of mean arterial pressure (MAP) and heart rate (HR) were derived from the signals of pulsatile arterial pressure. The cardiovascular parameters were recorded in conscious freely moving rats under normoxic conditions for 30 min. In the groups of rats used for verifying the reversibility of SH-induced cardiovascular changes, control and SH rats were initially submitted to experimental protocol and then submitted to the catheterization surgery. One day after the surgery, their cardiovascular parameters were evaluated as previously described. At the end of the experiments, the animals were sacrificed with an overdose of anesthesia (pentobarbital, 100 mg/kg).

Power spectral analyses of systolic arterial pressure and heart rate. Oscillations of arterial pressure and heart rate at low-frequency range (LF) are representative of the modulatory effects of sympathetic activity controlling vascular tonus and heart activity, while oscillations at high-frequency range (HF) are associated with a respiratory or parasympathetic modulation of blood vessels and the heart, respectively (Malliani *et al.* 1991; Bernardi *et al.* 2001; Zoccal *et al.* 2009*a*). In the present study, the magnitudes of autonomic and respiratory modulatory effects on the cardiovascular system were evaluated in SH and control rats. To reach this goal, baseline cardiovascular recordings of pulsatile arterial pressure of control and SH rats were processed (Chart Pro, ADInstruments) and beat-by-beat time series of systolic arterial pressure (SAP) and HR were extracted. The overall variability of these series was assessed in the time and frequency domain using fast Fourier transform spectral analysis (Cardioseries Software v2.4, available on https://www.sites.google.com/site/cardioseries/home). The power of the oscillatory components obtained from rats of control and SH groups was quantified in two frequency bands: LF (0.20–0.75 Hz) and HF (0.75–3.0 Hz) (Cerutti *et al.* 1991; Malliani *et al.* 1991; Zoccal *et al.* 2009*a*). Oscillations lower than 0.20 Hz were not quantified.

Statistical analyses

The data are expressed as mean ± standard error of mean and compared using Student's unpaired *t* test or one-way ANOVA followed by a Bonferroni post test. Differences were considered statistically significant when $P < 0.05$.

Results

Alterations in the respiratory pattern induced by SH

In situ preparations of control rats exhibited an eupnoeic-like breathing pattern (Paton, 1996; St-John &

Paton, 2003), as illustrated in panel *Aa* of Fig. 1: (i) PN showed a ramping pattern of discharge; (ii) cVN presented an inspiratory component (coincident with PN burst) followed by a decrementing post-I discharge; (iii) HN expressed an incrementing pre-inspiratory discharge that started before (~200 ms) the onset of PN burst; and (iv) AbN exhibited a low-amplitude expiratory activity with a low post-I peak. In preparations of rats previously submitted to SH, we observed marked changes in their respiratory motor activity (Fig. 1*Ab*). AbN activity of SH rats was significantly enhanced, with a gradual emergence of a novel high-amplitude burst of activity during mid-expiration that displayed its peak during the late part of E2 phase (late-E), and terminated abruptly before PN discharge ($n = 21$, Fig. 1*Ab*). The occurrence of the AbN late-E bursts in SH rats was combined with alterations in the other respiratory motor outputs: (i) PN burst exhibited a non-ramping/square pattern of discharge with reduced time of inspiration (0.6 ± 0.03 *vs.* 0.33 ± 0.01 s; $n = 36$; $P < 0.0001$) and increased time of expiration (2.3 ± 0.09 *vs.* 3.3 ± 0.06 s; $n = 36$; $P < 0.0001$; Fig. 1*Aa* and *b*, and *Ba*); (ii) the onset of pre-inspiratory activities in HN (0.21 ± 0.01 *vs.* 0.38 ± 0.02 s; $n = 15$; $P < 0.0001$) as well as in cVN (0.33 ± 0.04 *vs.* 0.59 ± 0.04 s; $n = 12$; $P = 0.0028$) were enhanced (Fig. 1*Aa* and *b*, and *Bb* and *c*); and (iii) the amplitude (47.8 ± 1.1 *vs.* $21 \pm 3.1\%$; $n = 12$; $P < 0.0001$) and duration (1.98 ± 0.06 *vs.* 1.44 ± 0.07 s; $n = 12$; $P = 0.002$) of cVN post-I activity were reduced ($n = 12$; Fig. 1*Aa* and *b*, and *Bc* and *d*). These findings indicate that preparations of SH

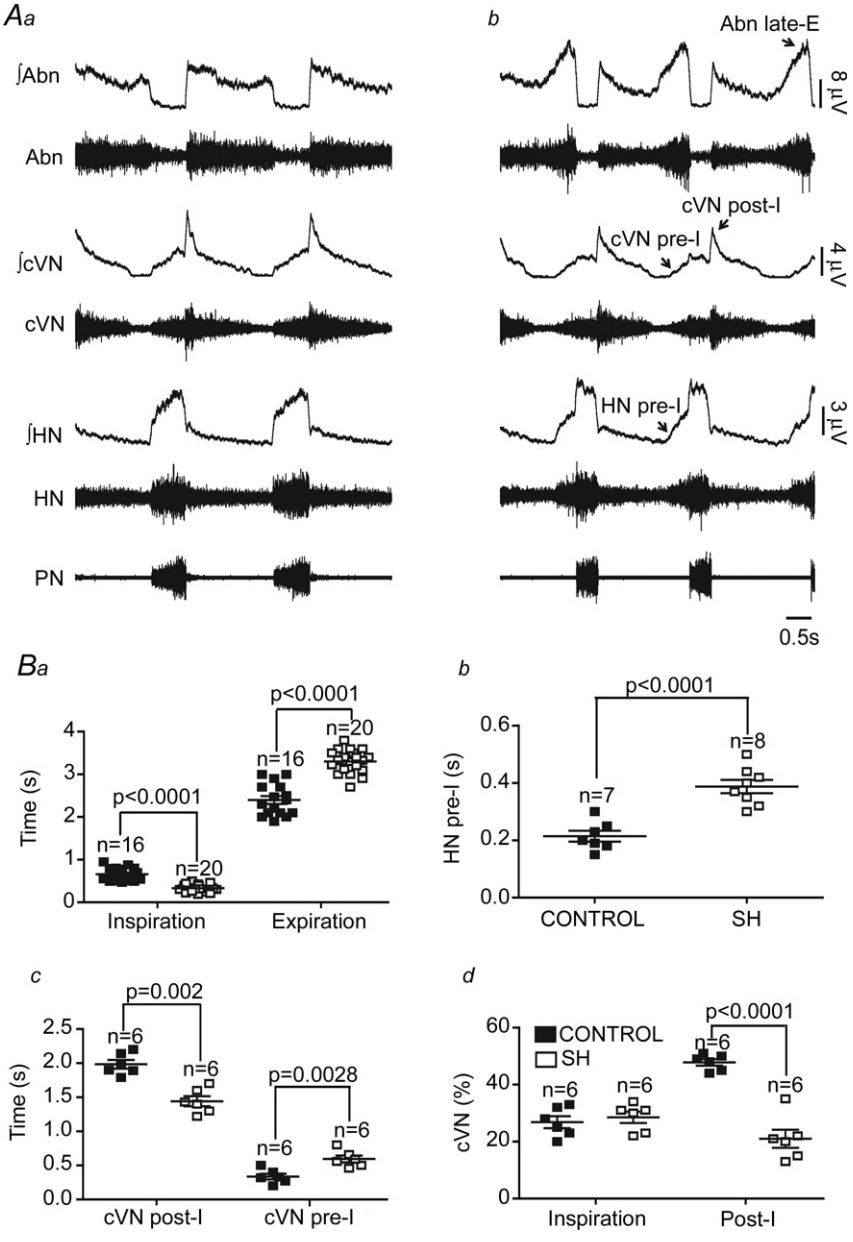

Figure 1. Respiratory motor activity after SH
Raw and integrated (∫) recordings of hypoglossal (HN), cervical vagal (cVN), abdominal (AbN) and phrenic (PN) nerve activities of a control (*Aa*) and a SH rat (*Ab*), representative of their respective groups. Average values of inspiratory and expiratory durations (*Ba*), HN pre-I duration (*Bb*), cVN pre-I and post-I duration (*Bc*) and cVN inspiratory and post-I magnitudes (*Bd*) of control and SH rats.

rats exhibit a pattern of active expiration, with recruitment of abdominal expiratory motor activity and correlated changes in the cranial motor outputs.

Subglottal pressure in control and SH rats

The impact of the changes in the pre-inspiratory and post-inspiratory activities induced by SH on the upper airway resistance was evaluated by measurements of subglottal pressure (SGP) in control ($n = 5$) and SH rats ($n = 5$). Figure 2 shows tracings of SGP from one control and one SH rat, representative of their respective groups. In control rats (Fig. 2*A*), SGP decreased before ($\Delta t = 0.11 \pm 0.04$ s; $\Delta P = 2.1 \pm 0.5$ mmHg) and during inspiration (coincident with PN burst), which corresponded to the dilatation of the vocal cords due to the contraction of abductor muscles. Immediately after inspiration, during the post-I phase, laryngeal adduction occurred and SGP increased ($\Delta P = 10 \pm 0.3$ mmHg). During the E2 phase, SGP values returned to baseline condition. In SH rats (Fig. 2*B*), the decrease in SGP occurred earlier ($\Delta t = 0.3 \pm 0.05$ s; $P = 0.0179$) with no changes in the magnitude of pressure reduction in comparison to control group ($\Delta P = 2.3 \pm 1$ *vs.* 2.1 ± 0.5 mmHg). During post-inspiration, the laryngeal adduction was significantly reduced in SH rats, leading to a diminished SGP during this phase ($\Delta P = 2.2 \pm 0.5$ *vs.* 10 ± 0.3 mmHg; $P < 0.0001$). These data indicate that upper airway resistance is reduced in SH rats during inspiration and expiration.

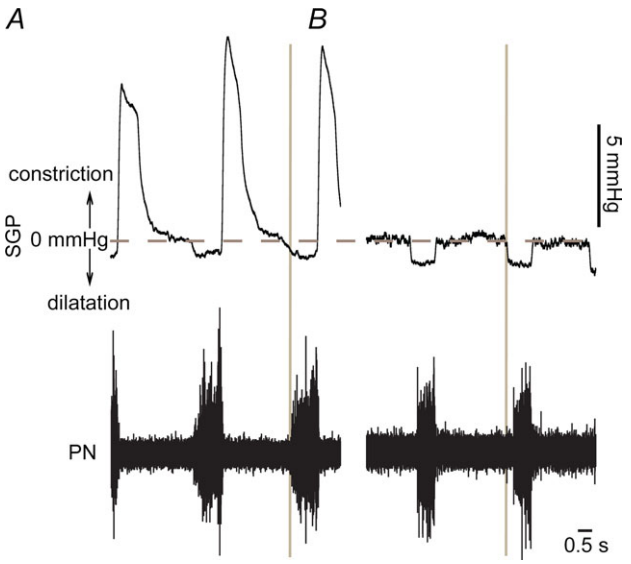

Figure 2. Measurements of subglottal pressure after SH
Simultaneous recordings of subglottal pressure, an index of upper airway resistance, and phrenic nerve activity (PN) of control (*A*) and SH (*B*) rats, representative of their respective groups. The vertical line indicates the moment when the upper airway resistance decreases before the onset of PN burst.

Effects of SH on the activity of the Bötzinger complex neurones

Considering that the expiratory motor activity was significantly changed in SH rats, we evaluated the activity of the BötC neurones, a major source of expiratory neurones in the brainstem (Ezure *et al.* 2003). Stable intracellular recordings of the post-I and aug-E neurones of the BötC were performed in control and SH rats to evaluate their membrane trajectory potential and intrinsic electrophysiological properties. As previous described (Smith *et al.* 2007), in the BötC of preparations of control rats ($n = 5$) post-I neurones displayed a decrementing pattern of discharge with a rapid depolarization at the end of inspiration (Fig. 3*Aa*). In SH rats ($n = 5$), the firing frequency of post-I neurones was significantly reduced in comparison to control group (97 ± 11 *vs.* 59 ± 9 Hz; $P < 0.001$; Fig. 3*Ab*). With respect to the membrane potential trajectories, post-I neurones from control rats showed two distinct periods of hyperpolarization: one coincident with a PN burst (ΔV: -19 ± 2 mV) and another during the E2 phase (ΔV: -5 ± 0.7 mV; Fig. 3*Aa*, *b* and *c*). Post-I neurones of SH rats displayed more negative membrane potential values during the E2 phase (-43 ± 2 *vs.* -55 ± 3 mV; $P = 0.0104$), with no changes during inspiration (-55 ± 2 *vs.* -56 ± 1.9 mV), in relation to control post-I neurones (Fig. 3*Ac*). After fast synaptic blockade, post-I neurones from control and SH groups exhibited similar values of intrinsic firing frequency (3.0 ± 0.2 *vs.* 3.2 ± 0.4 Hz), baseline membrane potential (-52 ± 2 *vs.* -55 ± 4 mV), input resistance (276 ± 8 *vs.* 273 ± 10 MΩ; Fig. 3*Ba*, *b* and *c*) and number of actions potentials in response to positive current injection (excitability; 100 pA: 25 ± 3 *vs.* 29 ± 5 spikes; $n = 10$; Fig. 3*Ca*, *b* and *c*).

The aug-E neurones in control group ($n = 5$; Fig. 4*Aa*) exhibited an augmenting pattern of discharge, starting during the E2 phase and ending before the PN burst (Smith *et al.* 2007). It was also possible to observe a period of hyperpolarization that initiated 40–70 ms before the PN burst and continued throughout the inspiratory phase (ΔV: -14 ± 3 mV). After inspiration, aug-E neurones of control rats depolarized slowly during the post-I phase, reaching a peak during the E2 phase with a consequent increased firing frequency (Fig. 4*Aa*). In SH rats ($n = 5$, Fig. 4*Ab*), the firing frequency of aug-E neurones was enhanced (31 ± 5 *vs.* 142 ± 9 Hz; $P < 0.0001$) in comparison to controls. However, the membrane potential of aug-E neurones from SH rats during the post-I (-47 ± 3 *vs.* -48 ± 4 mV) and inspiratory phases (-57 ± 3 *vs.* -56 ± 4 mV; Fig. 4*Ac*) were similar to aug-E neurones from control rats. After fast synaptic blockade, aug-E neurones from control and SH rats exhibited similar values of intrinsic firing frequency (39 ± 3 *vs.* 41 ± 5 Hz), baseline membrane potential

(50 ± 2 *vs.* 49 ± 3 mV), input resistance (286 ± 8 *vs.* 287 ± 5 MΩ; Fig. 4*Ba*, *b* and *c*) and number of actions potentials in response to positive current injection (excitability; 100 pA: 135 ± 7 *vs.* 129 ± 6 spikes; $n = 10$; Fig. 4*Ca*, *b* and *c*). These data indicate that SH rats present depressed post-I and increased aug-E neuronal activities in the BötC by mechanisms other than changes in their intrinsic electrophysiological properties.

Baseline sympathetic activity after SH

In addition to the respiratory activity, we also evaluated the level and pattern of baseline tSN activity in control and SH rats. In accordance with previous studies performed *in situ* (Zoccal *et al.* 2008) and *in vivo* (Malpas, 1998), the pattern of tSN activity in preparations from the control group ($n = 9$) showed a marked increase of activity

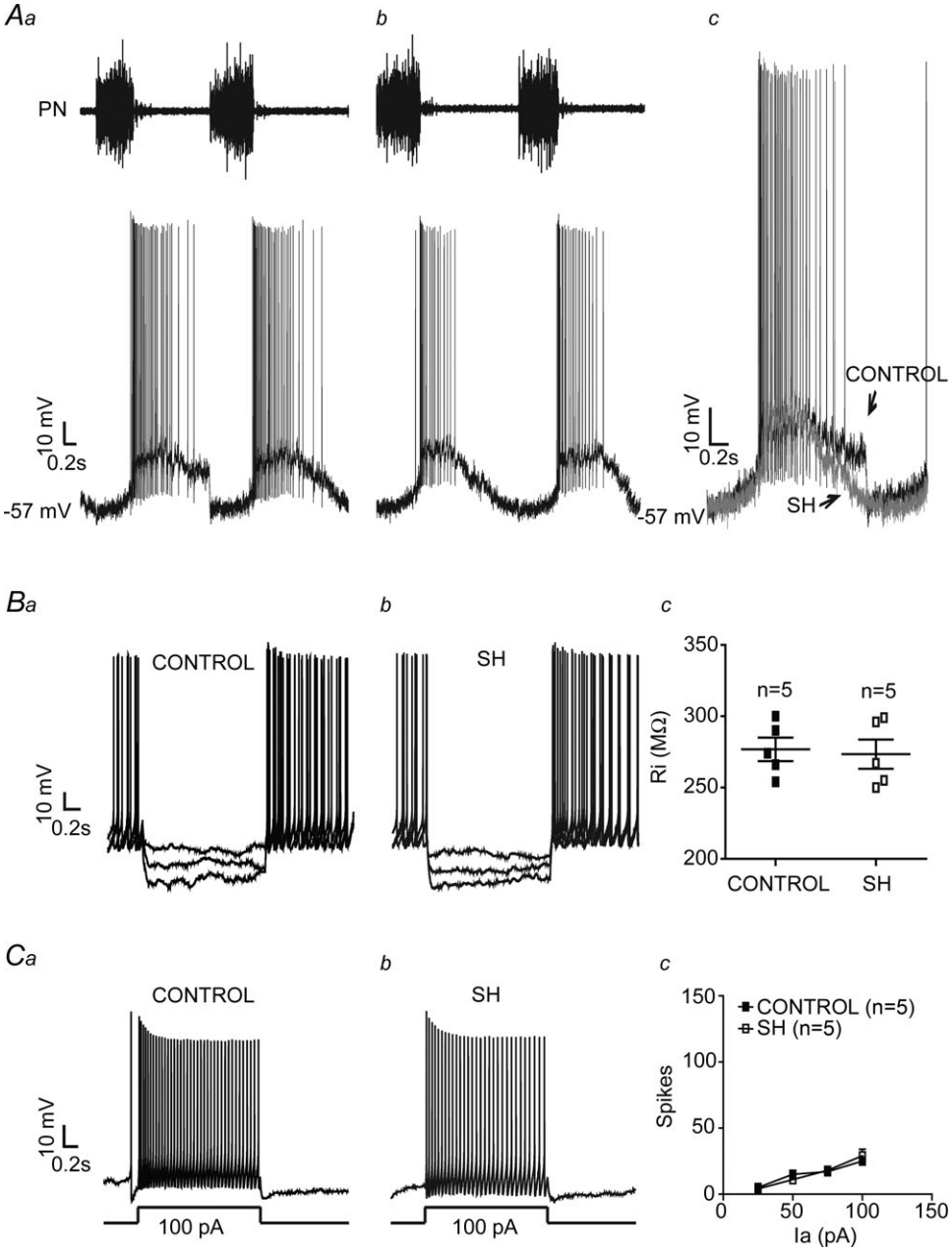

Figure 3. Intracellular recordings of BötC post-I neurones of control and SH rats
Simultaneous recordings of the activity of phrenic nerve (PN) and BötC post-I neurones of control (*Aa*) and SH rats (*Ab*), representative of their respective groups. In *Ac*, the intracellular recordings of post-I neurones of control and SH rats are superimposed. Note that the firing frequency of the post-I neurone of SH rat is reduced in comparison to control. In the presence of fast synaptic blockade, input resistance (R_i; *Ba*, *b* and *c*) and intrinsic excitability (*Ca*, *b* and *c*) were not different between control and SH rats. Ia: Current.

during the inspiratory phase, with peak activity at the end of inspiration/start of expiration (Fig. 5*A*). In SH rats ($n = 11$) an inspiratory/post-inspiratory sympathetic peak every respiratory cycle was also observed. However, the tSN of SH rats expressed an additional peak of discharge during the late-E period, which was not present in the control rats (Fig. 5*B*). Consequently, the levels of tSN of SH rats during the E2 phase (24.4 ± 2.3 *vs.* 45.6 ± 1.6%; $P < 0.0001$), but not during inspiratory (69 ± 1.3 *vs.* 67 ± 1.4%) and post-I phases (29 ± 1.3 *vs.* 28 ± 1.3%), were significantly higher than in controls (Fig. 5*A*, *B*, *C* and *D*). It is important to note that the emergence of late-E bursts in tSN of SH rats was phase-locked with the occurrence of late-E bursts in AbN (Fig. 5*C* and *D*). These data suggest that the central mechanisms generating the active expiration in SH rats also modulate the activity

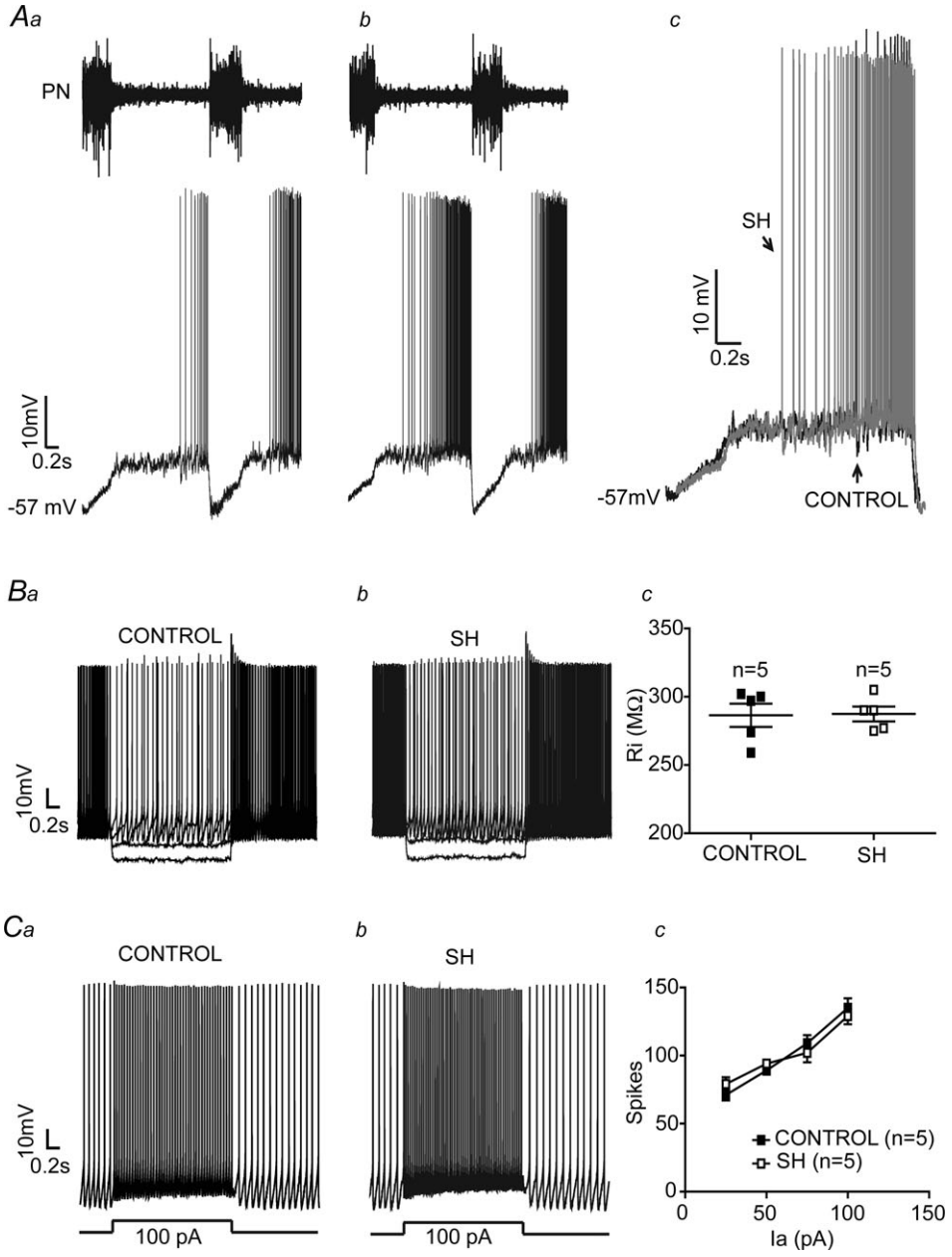

Figure 4. Intracellular recordings of BötC aug-E neurones of control and SH rats
Simultaneous recordings of the activities of phrenic nerve (PN) and BötC aug-E neurones of representative control (*Aa*) and SH (*Ab*) rats. In *Ac*, the intracellular recordings of aug-E neurones of control and SH rats are superimposed. Note that the aug-E neurone of SH rat displayed action potentials during mid-expiration whilst the control aug-E neurone fires only after the second half of expiration. In the presence of fast synaptic blockade, input resistance (*Ba*, *b* and c) and intrinsic excitability (*Ca*, *b* and c) were not different between control and SH rats. Ia: Current.

of RVLM pre-sympathetic neurones contributing to the observed increase in the sympathetic activity during the expiratory phase.

Impact of SH-induced late-E sympathetic overactivity on cardiovascular parameters

The cardiovascular implications of the emergence of late-E bursts in the sympathetic activity of SH rats were evaluated in the *in situ* preparations as well as in awake rats. In the *in situ* preparations, under the same conditions of flow rate, temperature and perfusate content, we verified that preparations of SH rats ($n = 20$) developed higher levels of perfusion pressure than preparations from the control rats ($n = 16$; 62 ± 1.5 *vs.* 76 ± 1.3 mmHg; $P < 0.0001$), indicating an increased vascular resistance in SH preparations (Fig. 6*A*, *B* and *C*). We also verified that the amplitude of Traube–Hering waves (increases in the arterial pressure generated every respiratory cycle; Simms

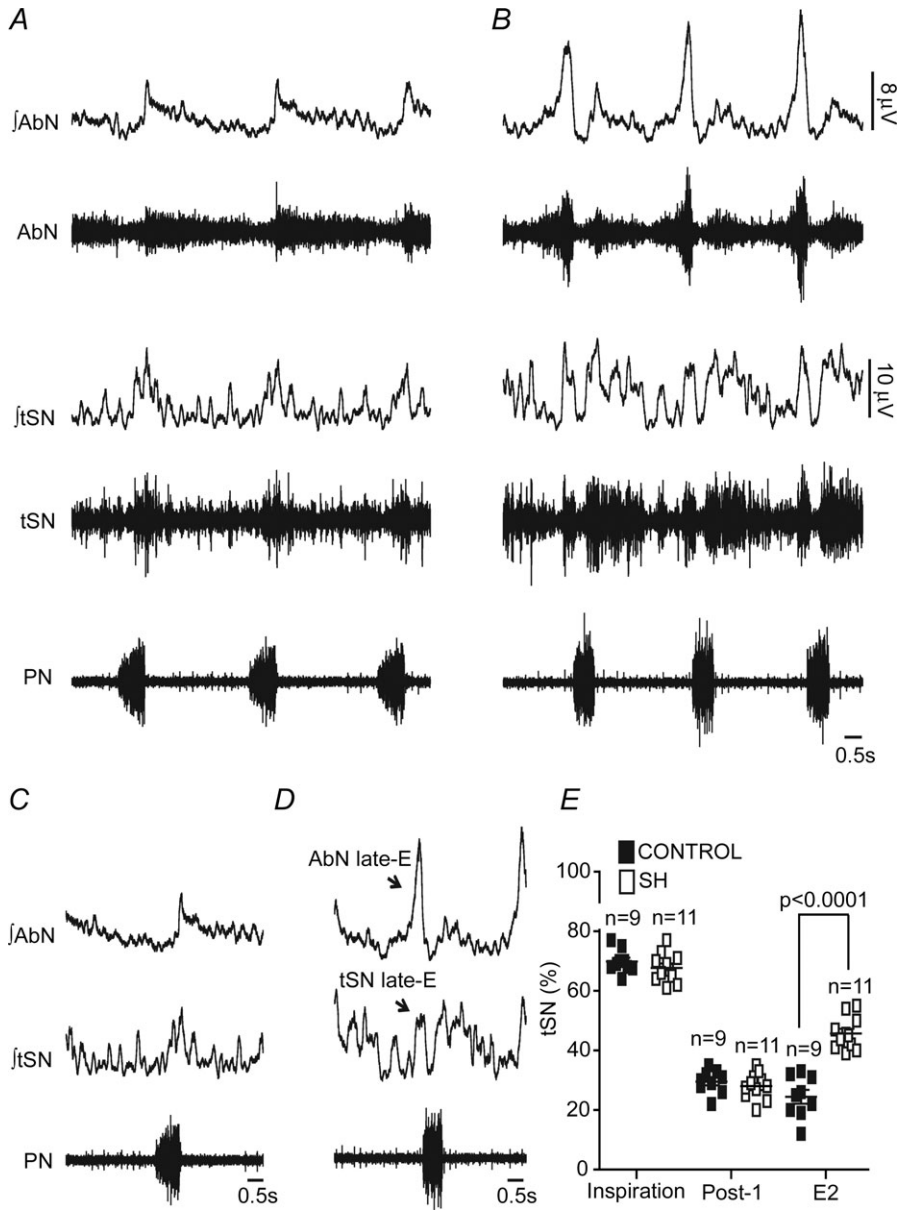

Figure 5. Respiratory–sympathetic coupling in SH rats
Raw and integrated (∫) recordings of abdominal (AbN), thoracic sympathetic (tSN) and phrenic nerve (PN) activities of control (*A*) and SH rats (*B*), representative of their respective groups. *C* and *D*, average AbN, tSN and PN recordings of control and SH rats illustrating the novel late-E component in the AbN and tSN of SH rat. *E*, average values of tSN of control and CIH rats during inspiration, post-inspiration and E2 phases.

et al. 2009; Moraes *et al.* 2012*b*) was higher in SH rats than in controls (2.6 ± 0.1 *vs.* 8 ± 0.3 mmHg; $n = 36$; $P < 0.0001$; Fig. 6*A*, *B* and *D*), indicating that the respiratory-related sympathetic overactivity of SH rats is transmitted to blood vessels of the *in situ* preparations.

In conscious freely moving rats, we verified that the baseline MAP of SH rats ($n = 21$) was significantly higher than in control rats ($n = 21$; 86 ± 2 *vs.* 97 ± 2 mmHg; $P = 0.0004$; Fig. 7*A*), while baseline HR was similar between groups (484 ± 13 *vs.* 490 ± 19 beats min^{-1}; Fig. 7*B*). With respect to the variability in the time domain, both SAP (21.8 ± 3.0 *vs.* 34.6 ± 1.8 mmHg^2; $P = 0.0009$; Fig. 7*C*) and HR variances (592.6 ± 51.9 *vs.* 822.2 ± 86.4 (beats min^{-1})^2; $P = 0.0345$; Fig. 7*D*) of SH rats were greater in comparison to control rats. Regarding the frequency domain analysis, SAP of SH rats displayed an augmented magnitude of the oscillatory components at low- (2.22 ± 0.25 *vs.* 5.20 ± 0.79 mmHg^2; $P = 0.0013$) and high-frequency ranges (1.80 ± 0.17 *vs.* 4.29 ± 0.87 mmHg^2; $P = 0.0099$) in comparison to controls (Fig. 7*E* and *G*), showing that SAP of SH rats exhibited a clear amplification in the sympathetic and respiratory modulation. These data show that SH produces a significant increase in baseline arterial pressure combined with augmented sympathetic- and respiratory-mediated modulatory effects on blood vessels. Similar to SAP, the magnitude of oscillatory low- (8.25 ± 1.18 *vs.* 23.20 ± 5.69 (beats min^{-1})^2; $P = 0.0171$) and high-frequency components (26.46 ± 3.62 *vs.* 52.20 ± 7.54 (beats min^{-1})^2; $P = 0.0047$) of HR in SH rats were significantly elevated in comparison to rats from control group (Fig. 7*F* and *H*). However, the cardiac LF/HF ratio (an index of sympathetic/parasympathetic balance to the heart) was not statistically different between groups (0.35 ± 0.05 *vs.* 0.49 ± 0.07; $n = 42$), suggesting that, in spite of the increased sympathetic and parasympathetic modulation to the heart, the cardiac autonomic balance was not altered by SH.

Effects of SH on the activity of RVLM pre-sympathetic neurones

We also evaluated whether the expiratory-related sympathetic overactivity of SH rats was consequent to changes in the intrinsic electrophysiological properties of bulbospinal pre-sympathetic neurones of the RVLM (Ross *et al.* 1984). To reach this goal, we performed intracellular recordings of RVLM pre-sympathetic neurones in control and SH rats. In accordance with previous studies (Haselton & Guyenet, 1989), in preparations of control rats ($n = 6$), we found a population of barosensitive (Fig. 8*Ac*) spinally projecting (latency: 4.8 ± 0.9 ms; Fig. 8*Ad*) RVLM pre-sympathetic neurones that exhibited an irregular firing frequency with positive post-inspiratory pattern of discharge (Fig. 8*Aa*). In the RVLM of SH rats ($n = 5$), we recorded a similar population of pre-sympathetic neurones that exhibited a post-inspiratory pattern of discharge, but also displayed an enhanced frequency of discharge during the late-E phase

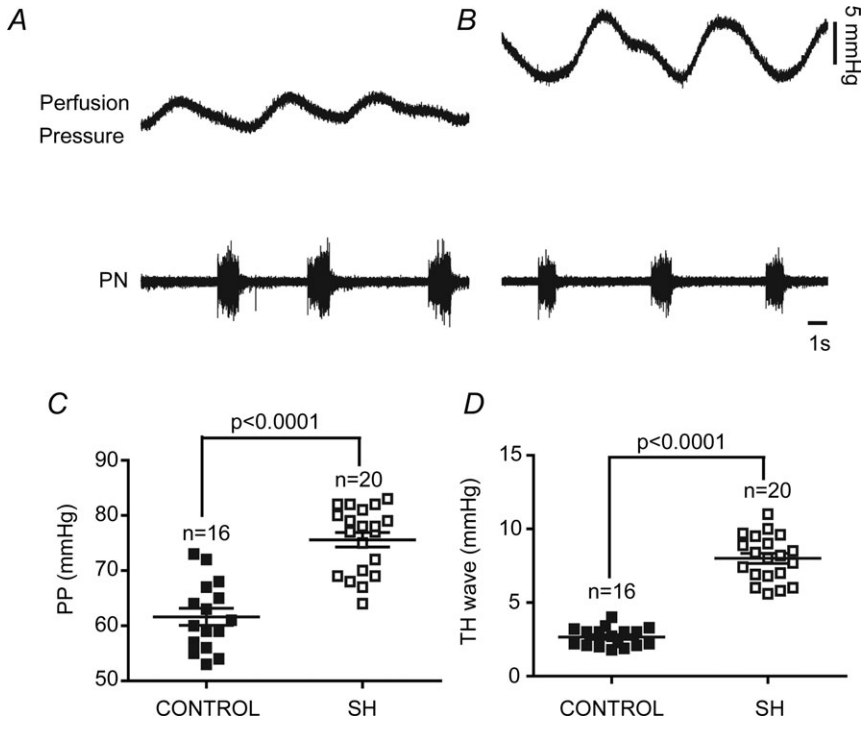

Figure 6. Amplified Traube–Hering waves of *in situ* preparations of SH rats
Recordings of perfusion pressure (PP) and PN activities of representative control (*A*) and SH rats (*B*). *C* and *D*, average values of PP and the magnitude of Traube–Hering waves (TH waves), respectively, in control and SH rats.

(34 ± 3 *vs.* 50 ± 4 Hz; $P = 0.0098$), as demonstrated in Fig. 8*Ab*. After the blockade of fast synaptic transmission, the RVLM pre-sympathetic neurones of control and SH rats showed similar values of intrinsic firing frequency (15 ± 4 *vs.* 17 ± 6 Hz; Fig. 8*Ae* and *f*), baseline membrane potential (54 ± 4 *vs.* 56 ± 7 mV), input resistance (233 ± 11 *vs.* 243 ± 7 MΩ; Fig. 8 *Ba*, *b* and *c*) and the number of action potentials in response to positive current injection (excitability; 25 pA: 32 ± 4 *vs.* 26 ± 5 spikes; Fig. 8*Ca*, *b* and *c*). These data indicate that the SH-induced increased sympathetic activity during E2 is associated with an enhanced firing frequency of pre-sympathetic neurones during late-E phase. This expiratory-related excitation of pre-sympathetic neurones of SH rats is independent of changes in their intrinsic electrophysiological properties and seems to be associated with an augmented excitatory drive to the RVLM.

Contribution of glutamatergic neurotransmission in the BötC/RVLM region to the generation of active expiration and sympathetic overactivity in SH rats

Considering that the activity of BötC and RVLM neurones are altered in SH rats by mechanisms not involving changes in their intrinsic electrophysiological properties, herein we evaluated the possible changes in the respiratory and sympathetic activities in response to the antagonism of ionotropic glutamate receptors in the BötC/RVLM region of SH rats. After bilateral microinjections of kynurenic acid into the BötC/RVLM (Fig. 9*Aa* and *b*), the eupnoeic-like pattern was restored in SH rats: (i) late-E bursts in AbN were eliminated ($n = 6$; Fig. 9*Ba*, *b* and *c*); (ii) PN recovered its ramping pattern of discharge (time of inspiration: 0.65 ± 0.03 *vs.* 0.68 ± 0.02 s for control and SH rats, respectively, 15 min after microinjections of kynurenic acid; $n = 22$; Fig. 9*Ba* and *b*; Fig. 10*A*);

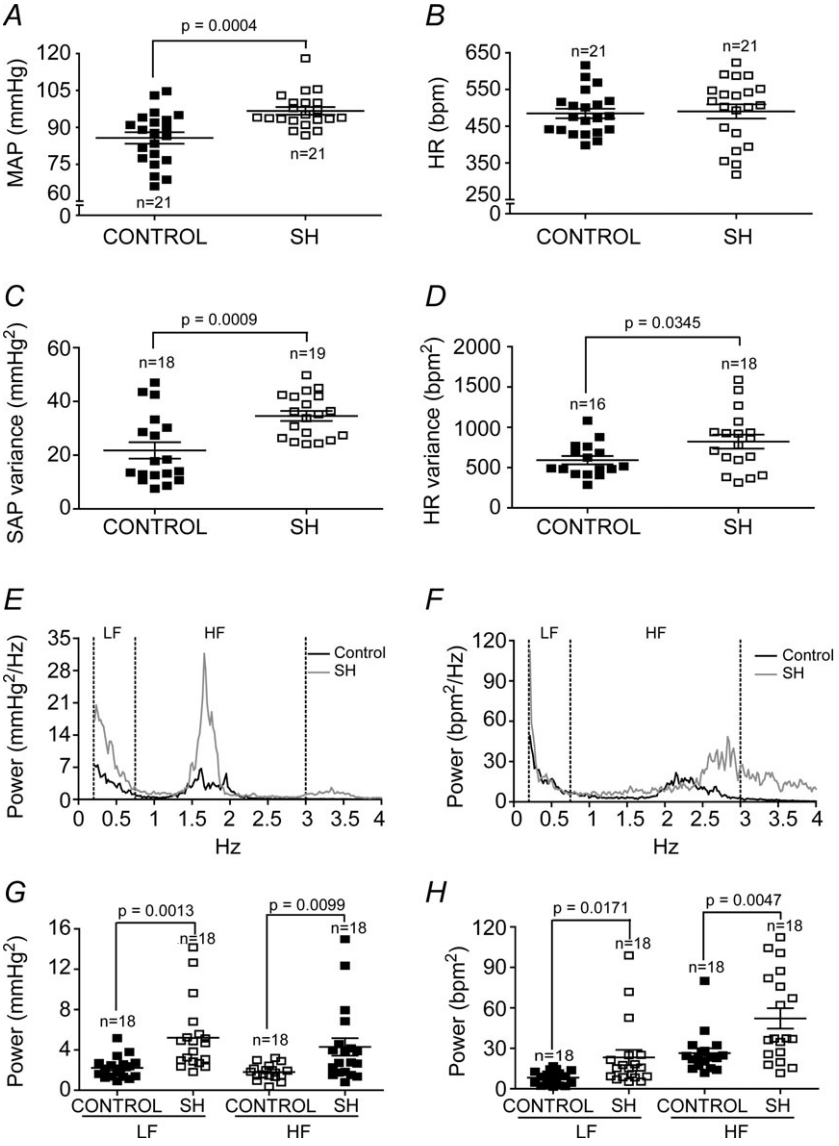

Figure 7. Cardiovascular parameters in conscious freely moving SH rats
Average values of baseline mean arterial pressure (MAP, *A*) and heart rate (HR (beats min^{-1}), *B*); systolic arterial pressure (SAP, *C*) and heart rate (HR, *D*) variances; systolic arterial pressure (SAP, *E*) and heart rate (HR, *F*) frequency spectra of representative rats; and the magnitude of low- (LF) and high-frequency (HF) components of SAP (*G*) and HR (*H*) of control and SH rats.

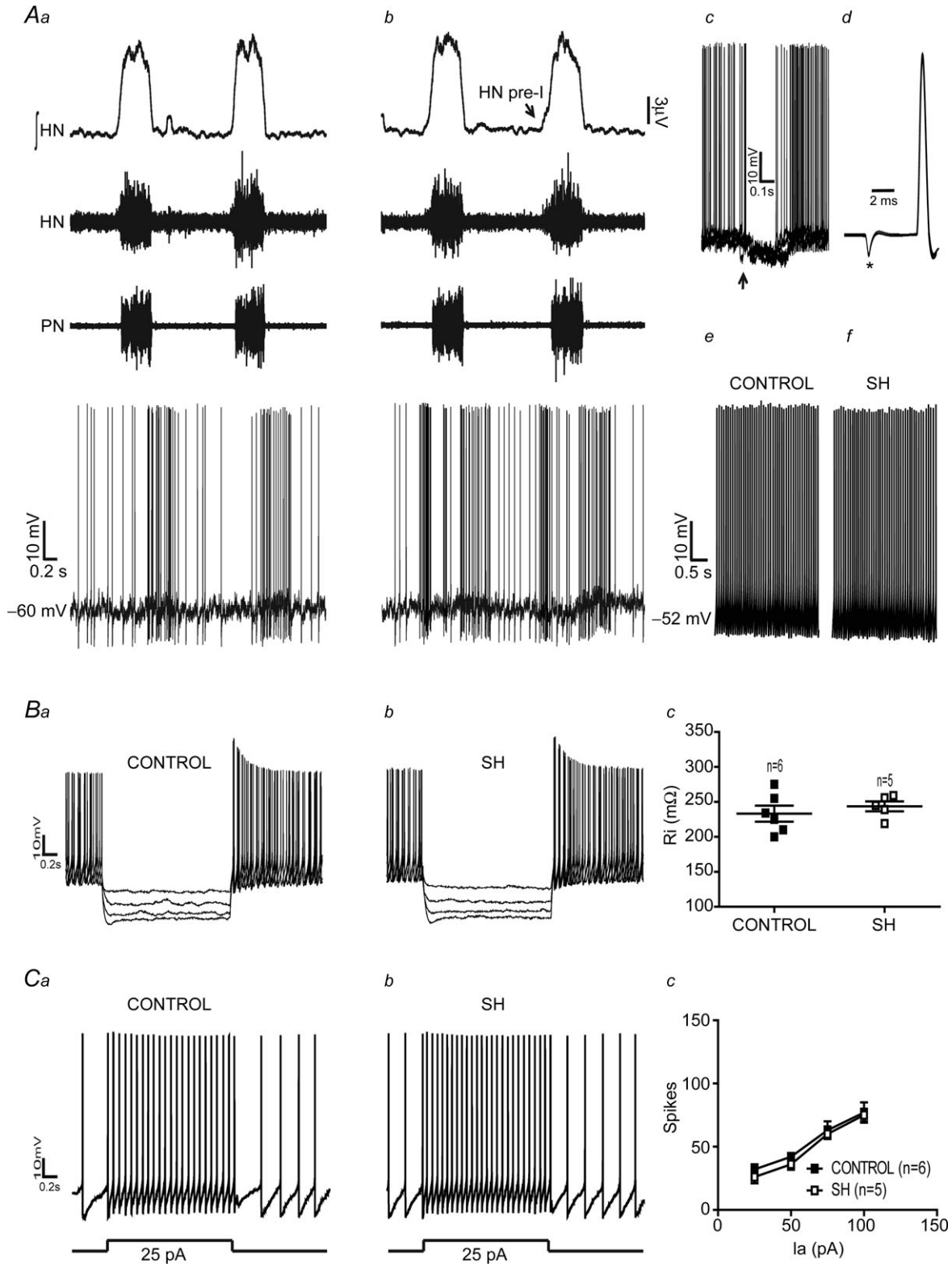

Figure 8. Effects of SH on the RVLM pre-sympathetic neurones
Simultaneous recordings of the activity of hypoglossal nerve (HN), phrenic nerve (PN) and RVLM neurones of control (*Aa*) and SH rats (*Ab*), representative of their respective groups. These neurones were inhibited during baroreflex activation (↑; *Ac*) and spinal stimulation (∗; *Ad*) evoked constant latency antidromic spikes. Note that RVLM neurone of SH rat displayed an increased frequency discharge during late-E. In the presence of fast synaptic blockade, the intrinsic firing frequency (*Ae* and *f*), input resistance (*Ba*, *b* and *c*) and intrinsic excitability (*Ca*, *b* and *c*) of RVLM pre-sympathetic neurones of SH rats were not different from controls. Ia: Current.

(iii) HN pre-inspiratory (pre-I) activity was normalized (pre-I duration: 0.21 ± 0.01 *vs.* 0.28 ± 0.02 s for control and SH rats, respectively, 15 min after microinjections of kynurenic acid; $n = 10$; Fig. 10*B*), and (iv) cVN post-I activity was enhanced (47.8 ± 1.1 *vs.* 47.3 ± 2.8% for control and SH rats, respectively, 15 min after kynurenic acid microinjections; $n = 9$; Fig. 10*C*). These data show that the antagonism of ionotropic glutamate receptors in the BötC/RVLM region eliminated the SH-induced active expiratory pattern and restored the normal breathing pattern, similarly to that observed in controls. In addition to the reduction of expiratory activity and recovery of a eupnoeic-like breathing pattern, microinjections of kynurenic acid into the BötC/RVLM region abolished the emergence of late-E bursts in tSN (24.4 ± 2.3 *vs.* 27.1 ± 2.3%, control and SH rats, respectively, 15 min after microinjections of kynurenic acid; $n = 15$; Figs 9*Ba*, *b* and *c* and 10*D*). Therefore, the activation of glutamatergic ionotropic receptors at the level of BötC/RVLM is critical for the generation of coupled active expiration and sympathetic overactivity in SH rats.

Effects of SH on the activity of RTN/pFRG late-E neurones

Previous studies documented that the RTN/pFRG region contains expiratory neurones, named late-E neurones (Abdala *et al.* 2009; Pagliardini *et al.* 2011; Moraes *et al.* 2012*a*), which may provide the excitatory drive to generate coupled late-E bursts in abdominal and sympathetic activities (Molkov *et al.* 2011). For this reason we hypothesized that the activity of the RTN/pFRG late-E neurones

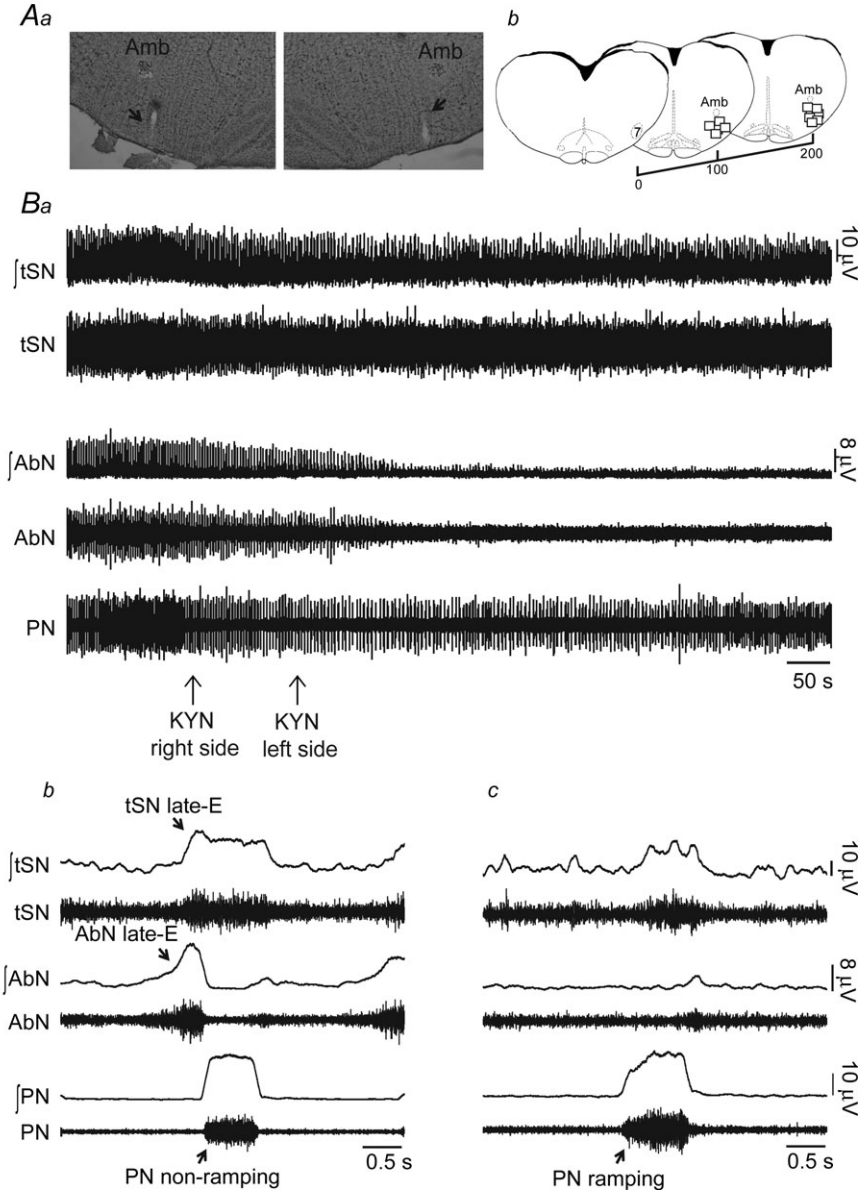

Figure 9. Glutamatergic transmission in the BötC/RVLM of SH rats
Aa, photomicrography of a coronal section of a brainstem from a SH rat, representative of the group, illustrating the pipette track in the region of BötC/RVLM. *Ab*, schematic drawings of coronal brainstem sections showing the sites of microinjections into the BötC/RVLM of SH animals. All bilateral microinjections are shown on the same side of representation. Amb: Nucleus Ambiguus *Ba*, raw and integrated (∫) recordings of abdominal (AbN), thoracic sympathetic (tSN) and phrenic nerve activities of a SH rat, representative of the group, illustrating the effects of bilateral microinjections of kynurenic acid (KYN) into the BötC/RVLM region. *Bb* and c, cycle-triggered averages of tSN, AbN and PN showing the pattern of respiratory and sympathetic activities before (*Bb*) and after (*Bc*) bilateral microinjections of KYN into the BötC/RVLM region.

is enhanced in response to SH. To test this hypothesis, we performed extracellular recordings of RTN/pFRG late-E neurones in control and SH rats. In control rats ($n = 5$), late-E neurones of the RTN/pFRG were silent at baseline conditions (normocapnia; Fig. 11*Aa*), while during hypercapnia (10% CO_2), the RTN/pFRG late-E neurones presented a rhythmic activity, exhibiting a rapid firing frequency exclusively during the end of expiration or late-E phase (45 ± 5 Hz), as illustrated in Fig. 11*Ab*. In SH rats ($n = 5$), we found that the late-E neurones of the RTN/pFRG displayed, at baseline conditions (normocapnia), rhythmic discharges during the late-E phase (39 ± 4 Hz; Fig. 11*Ac*) similar to controls during hypercapnia. These data indicate that the silent late-E neurones of the RTN/pFRG are active after SH, highlighting an important role of the RTN/pFRG region as a source of excitatory drive to generate the coupled late-E bursts in abdominal and sympathetic activities in SH rats.

Recovery of the SH-induced changes in the respiratory and sympathetic activities

Another group of SH rats was kept in normoxia for an additional 24 h after the end of the SH protocol to evaluate whether or not the active expiratory pattern and the sympathetic overactivity elicited by SH were maintained. The *in situ* preparations of these animals ($n = 15$) did not present the late-E bursts in AbN. Moreover, baseline PN (time of inspiration: 0.66 ± 0.05 *vs.* 0.61 ± 0.03 s; time of expiration: 2.3 ± 0.12 *vs.* 2.72 ± 0.12 s), HN (pre-I duration: 0.21 ± 0.01 *vs.* 0.23 ± 0.02 s), cVN (post-I activity: 47.8 ± 1.9 *vs.* 42.3 ± 3.7%) and tSN (E2 activity: 24.3 ± 2.2 *vs.* 29.1 ± 3.1%) were similar to controls ($n = 10$). In unanaesthetized conditions, SH rats maintained for 24 h in normoxia ($n = 18$) exhibited similar baseline MAP (89 ± 2 *vs.* 88 ± 2 mmHg), HR (475 ± 9 *vs.* 492 ± 10 beats min^{-1}) and SAP variability (LF: 3.47 ± 0.65 *vs.* 3.41 ± 0.58 $mmHg^2$; HF: 3.69 ± 0.43 *vs.* 3.73 ± 0.79 $mmHg^2$) in comparison to control rats ($n = 17$). These data show that the active expiration and sympathetic overactivity induced by SH were reversible after 24 h of normoxia.

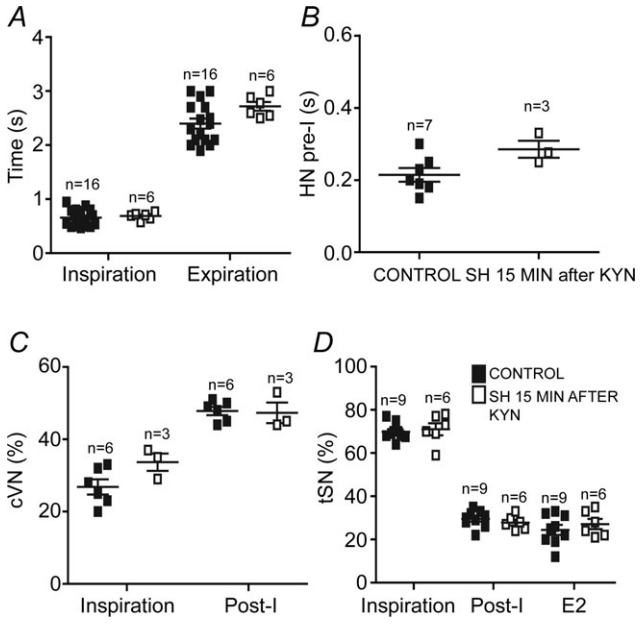

Figure 10. Changes in respiratory and sympathetic activities induced by bilateral microinjections of kynurenic acid into the BötC/RVLM region of SH rats
Average values of time of inspiration and expiration (*A*), HN pre-I duration (*B*), magnitude of inspiratory and post-inspiratory components of cVN (*C*) and tSN activities (*D*) during inspiration, post-inspiration and E2 phases in control rats and in SH rats after the antagonism of ionotropic glutamatergic receptors in the BötC/RVLM.

Discussion

Experimental evidence indicates that SH produces important functional changes in the respiratory and cardiovascular systems, including increases in baseline

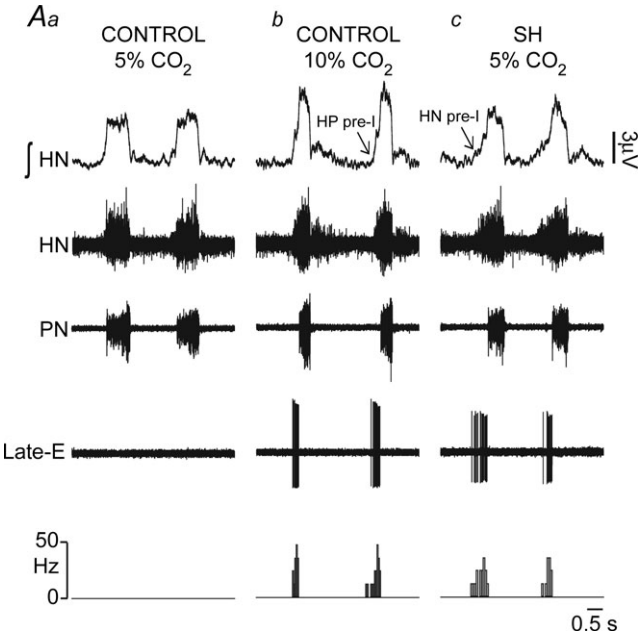

Figure 11. Extracellular recordings of RTN/pFRG late-E neurones of control and SH rats
Simultaneous recordings of hypoglossal nerve (HN), phrenic nerve (PN) and RTN/pFRG late-E activities of control (*Aa* and *b*) and SH rats (*Ac*), representative of their respective groups, in different levels of CO_2 (5 and 10%). At the bottom a histogram shows the frequency of late-E neurones (bin size: 85 ms). Note that the late-E neurone of control rat was silent in normocapnic conditions (5% CO_2) but became rhythmically activated in conditions of hypercapnia (10% CO_2). In contrast, the late-E neurone of SH rat exhibited rhythmic discharges in conditions of normocapnia.

minute ventilation (Powell *et al.* 1998) and arterial pressure (Rostrup, 1998; Calbet, 2003). However, an evaluation of respiratory and sympathetic vasoconstrictor motor outputs and the assessment of the neuronal mechanisms underpinning the cardiorespiratory changes induced by SH were not performed before the present study. Therefore, we are presenting novel data about the neural and motor adaptations of respiratory and sympathetic systems in response to short-term SH (24 h). Using a decerebrated arterially perfused *in situ* preparation in rat, we verified that SH exposure transformed the expiration into an active process, accompanied by the following neural changes: (i) AbN showed an additional burst of activity during late-E; (ii) HN and cVN pre-I activities were enhanced; and (iii) cVN post-I activity was depressed. In addition, SH rats also presented an augmented sympathetic activity during the E2 phase coupled with the emergence of late-E bursts in AbN, associated with high amplitude Traube–Hering pressure waves in the *in situ* preparations, and increased baseline arterial pressure in conscious freely moving rats. We are also describing that the expiratory neurones of BötC and the pre-sympathetic RVLM neurones of SH rats presented marked changes in their firing frequency, which were not due to changes in their intrinsic electrophysiological properties but rather dependent on glutamatergic synaptic inputs from other brainstem areas, including the RTN/pFRG. With this body of experimental evidence, we show for the first time that the short-term SH produces changes in medullary respiratory and sympathetic neurones, generating an active expiratory pattern coupled to an increased sympathetic activity. Whether or not there is a cause–effect relationship between these two phenomena in SH rats is still a matter for further investigation.

SH induces active expiration

The most evident alteration in the respiratory motor activity of SH rats was the emergence of high-amplitude bursts in AbN during the late part of the E2 phase. Late-E activity in AbN is associated with an active expiratory pattern (Janczewski & Feldman, 2006; Pagliardini *et al.* 2011), as observed in conditions of hypercapnia (Abdala *et al.* 2009), acute activation of peripheral chemoreceptors (Moraes *et al.* 2012*a*) or in rats submitted to chronic intermittent hypoxia (Zoccal *et al.* 2008). Combined with the increased AbN motor activity, SH rats also exhibited enhanced/anticipated pre-I activities in HN and cVN and a reduced post-I activity in cVN. The pre-I activity of HN and cVN is associated with contractions of genioglossus and upper airway abductor muscles, respectively, while the expiratory motor fibres of cVN control the activity of adductor glottis muscle (Paton & Dutschmann, 2002). Based on these findings, we suggest that the increased HN and cVN pre-I activities of SH rats were responsible for the anticipatory upper airway dilatation, before the onset of inspiration, while the reduced post-I component of cVN activity resulted in a decreased subglottal pressure during expiration. The reduced airflow resistance during expiration of SH rats, in combination with the recruitment of the abdominal expiratory muscles, may be considered as an important motor adaptation contributing to increase pulmonary gas exchange, as part of the ventilator adaptation to SH (Aaron & Powell, 1993).

The firing frequency of BötC post-I neurones from SH rats was significantly reduced in comparison to controls. Although the phenotype of the neurones recorded (excitatory or inhibitory, Rybak *et al.* 2004) was not determined, we suggest that the depressed BötC post-I activity is the cause of cVN post-I activity reduction. The analyses of intrinsic electrophysiological properties indicated that the SH-induced post-I neuronal depression was dependent on synaptic inputs, rather than alterations in their neuronal excitability. Different from post-I neurones, we verified that the activity of BötC aug-E neurones was significantly enhanced in SH rats. The excitabilities of aug-E neurones of SH and control rats were similar, indicating that synaptic inputs critically contribute to the observed changes in aug-E neurones of SH rats. In this scenario, we verified that the antagonism of ionotropic glutamatergic receptors in the BötC restored the post-I activity and the eupnoeic-like breathing pattern of SH rats. It is important to note that this pattern of response is different from that observed in control rats, as demonstrated in a previous study from our laboratory (Moraes *et al.* 2012*c*). These findings indicate that SH may facilitate the glutamatergic transmission at the level of BötC, which appears to be critical to change the activity of expiratory neurones in this region. Considering previous studies suggesting that aug-E and post-I neurones of the BötC may establish reciprocal inhibitory synapses (Shen *et al.* 2003; Smith *et al.* 2007), and our results showing that the membrane potential of post-I neurones of SH rats showed an early hyperpolarization phase-locked with the anticipated depolarization of aug-E neurones, we hypothesize that the glutamatergic transmission is important to increase the activity of aug-E neurones that, in turn, depress the activity of post-I neurones. With these data we are not able to elucidate the sources of glutamatergic drive inducing the changes in the BötC neuronal activity of SH rats, but we suggest that it arises from pontine respiratory neurones (Smith *et al.* 2007) as well as from neurones of the commissural nucleus tractus solitarii receiving inputs from the peripheral chemoreceptors (Takakura *et al.* 2006; Moraes *et al.* 2012*c*).

The antagonism of glutamatergic transmission in the BötC of SH rats restored the HN pre-I activity, suggesting that the SH-induced changes in the BötC activity also

affected the neuronal activity of other sub-regions of ventral respiratory column (VRC). The possibility that these effects are due to the spreading of the glutamate receptor antagonist from the BötC to other sub-regions of the VRC is very low, because in a previous study we demonstrated that it is possible to target selectively different sub-regions of the VRC (Moraes *et al.* 2012*c*). Therefore, our data indicate that the glutamate-mediated alterations in the BötC neuronal activity of SH rats are important to change the activity of inspiratory neurones of VRC.

In the present study we documented that expiratory neurones of the RTN/pFRG from SH rats were active at basal conditions. Previous studies reported that the RTN/pFRG contains silent late-E neurones that present oscillatory activity in conditions of hypercapnia, activation of peripheral chemoreceptors or reduced inhibitory transmission (Abdala *et al.* 2009; Pagliardini *et al.* 2011; Moraes *et al.* 2012*a*). In addition, the emergence of late-E activity in RTN/pFRG was coincident with the presence of late-E bursts in abdominal motor activity (Abdala *et al.* 2009; Pagliardini *et al.* 2011; Moraes *et al.* 2012*a*), suggesting a causal relationship between RTN/pFRG activation and active expiration. The data showing that the RTN/pFRG late-E neurones were active at basal conditions suggest that this region contributes to the emergence of an active expiratory pattern in SH rats. We still do not have experimental evidence characterizing the phenotype of RTN/pFRG late-E neurones as well as their connectivity with the respiratory central pattern generator. Therefore, it remains to be elucidated how RTN/pFRG late-E neurones interact with the VRC and activate pre-motor expiratory neurones and generate late-E bursts in AbN (Bochorishvili *et al.* 2012). In spite of this limitation, we suggest the following possible mechanisms to explain the emergence of RTN/pFRG late-E neuronal activity in SH rats at baseline conditions: (a) changes in intrinsic neuronal electrophysiological properties, (b) enhanced central or peripheral chemoreceptor drive (Molkov *et al.* 2011), and (c) changes in pontine respiratory activity (Abdala *et al.* 2009). Considering that microinjections of glutamatergic receptor antagonist into the BötC eliminated the late-E bursts in abdominal nerve, we cannot exclude the possibility that interactions between BötC and RTN/pFRG may also contribute to the emergence of late-E activity (Rosin *et al.* 2006; Molkov *et al.* 2010). It is important to note that all these hypotheses require additional experiments to be tested.

Sympathetic overactivity induced by SH

Studies performed in humans documented an increase in arterial pressure and noradrenaline spillover in response to SH (Rostrup, 1998; Calbet, 2003; Gilmartin *et al.* 2008), suggesting that SH increases sympathetic outflow. Indeed, Hansen & Sander (2003) demonstrated that healthy humans sojourning in high altitudes for 4 weeks presented an augmented muscle sympathetic nerve activity that lasted for at least 3 days after their return to sea level. In the present study, we demonstrated that rats submitted to SH for 24 h presented an elevated baseline sympathetic activity coincident with high levels of perfusion pressure in the *in situ* preparations as well an augmented baseline arterial pressure and sympathetic-related (LF) variability in conscious rats. These findings indicate that SH produces a persistent activation of the sympathetic nervous system, which seems to be the cause of the increase in arterial blood pressure.

The analyses of sympathetic discharge pattern revealed that augmented sympathetic outflow of SH rats was coupled with the emergence of active expiration. The enhanced late-E sympathetic activity observed in SH rats potentially underpinned the augmented Traube–Hering waves in the *in situ* preparations as well as the increased respiratory-related (HF) variability of arterial pressure of conscious rats. We also found that the RVLM pre-sympathetic neurones exhibited an increased frequency of discharge during late-E, which correlated with the late-E bursts in sympathetic nerve activity. The changes in the frequency of discharge of RVLM pre-sympathetic neurones appeared to be dependent on excitatory synaptic inputs rather than changes in their intrinsic activity. In fact, the antagonism of ionotropic glutamatergic receptors with kynurenic acid in the RVLM of SH abolished the late-E bursts in tSN, indicating that the glutamatergic neurotransmission is critical for the generation of late-E depolarization in pre-sympathetic neurones of SH rats. These effects of microinjections of kynurenic acid in the RVLM of SH rats are different from those reported previously in control rats, in which a depression of inspiratory/post-inspiratory modulation of sympathetic nerve activity was observed (Guyenet *et al.* 1990; Koshiya *et al.* 1993; Moraes *et al.* 2012*c*). These differences may indicate that the late-E glutamatergic inputs to RVLM neurones are not presented in control rats at baseline conditions and emerge after exposure to SH. Therefore, our data pointed to two novel and important findings: (i) the development of sympathetic overactivity of SH rats is coincident with the generation of an active expiratory pattern; and (ii) expiratory-modulated excitatory inputs to pre-sympathetic RVLM neurones are required for the emergence of late-E bursts in the sympathetic activity of SH rats.

In the context of the scenario described above, we suggest that the active late-E neurones of RTN/pFRG of SH rats may be the source of increased glutamatergic inputs to RVLM pre-sympathetic neurones (Molkov *et al.* 2011). This possibility may explain the generation of coupled active expiration and sympathetic late-E bursts of SH rats. On the other hand, we cannot exclude the possibility that

the late-E modulation of RVLM pre-sympathetic neurones of SH rats is driven by BötC aug-E neurones that may establish synaptic contacts with the pre-sympathetic neurones (Sun *et al.* 1997). The pontine respiratory neurones should also be considered because of their important role in the generation of respiratory–sympathetic coupling (Baekey *et al.* 2008) and for the active expiratory pattern (Abdala *et al.* 2009). Our findings demonstrated that the development of sympathetic overactivity in SH rats is critically associated with the occurrence of ventilatory changes, mainly with the emergence of active expiration. This expiratory-modulated sympathetic overactivity developed by SH rats appears to be critical to elevate baseline arterial pressure and enhance the variability at low- (sympathetic-mediated) and high-frequency (respiratory-mediated) ranges. However, further functional and anatomical experiments are also needed to evaluate all these possibilities.

Physiological relevance of changes in the coupling of active expiration and sympathetic activity after SH

In conditions of SH, as experienced at high altitudes, a time-dependent increase in ventilation, namely ventilatory acclimatization to hypoxia (Powell *et al.* 1998) is observed. In the present study we characterized the respiratory motor changes induced by short-term SH, demonstrating that rats submitted to this condition presented a pattern of active expiration combined with a reduced upper airway resistance during expiration. Entrained with the generation of active expiratory pattern, we demonstrated that SH elevated baseline sympathetic activity and increased arterial pressure. The augmented sympathetic activity of SH rats, acting on the vascular smooth muscle of resistance vessels, may counteract the vasodilator effects elicited by hypoxaemia and the consequent rise in systemic arterial pressure levels may be important to prevent any reduction in the cerebral blood flow (Paton *et al.* 2009; Ainslie & Ogoh, 2010). Therefore, we suggest that the coupled increase in expiratory and sympathetic motor activities is part of a homeostatic adjustment to maintain proper arterial P_{O_2} and blood flow supply to body tissues and especially to the brain.

Our findings of coupled active expiration and sympathetic overactivity during the expiratory phase and augmented arterial pressure after SH are similar to those observed in hypertensive rats previously submitted to chronic intermittent hypoxia (CIH) for 10 days (Zoccal *et al.* 2008, 2009*a*). In CIH rats, we previously reported that the strengthened coupling between expiratory and sympathetic activity critically contributes to the development of sympathetic overactivity and maintenance of high blood pressure in this experimental model (Zoccal *et al.* 2009*a*; Molkov *et al.* 2011; Moraes *et al.* 2013). Based on this evidence, we suggest that the active expiration and sympathetic overactivity observed in SH rats contribute to the development of maladaptive cardiorespiratory responses to SH. This may be the case of individuals experiencing high altitude or mountain sickness, with the onset of pulmonary hypertension, pulmonary and cerebral oedema, and systemic hypertension (Hainsworth & Drinkhill, 2007). In both hypoxic conditions (sustained and intermittent), the carotid bodies play a critical role in eliciting the cardiorespiratory changes (Fletcher, 2001; Jacono *et al.* 2005). Therefore, we might expect that SH and CIH share common central mechanisms to generate late-E bursts in abdominal and sympathetic activities.

In the present study we also observed that the altered respiratory pattern and arterial pressure of SH rats returned to control levels when the animals were maintained in normoxia for an additional 24 h after the SH protocol. In contrast, in CIH rats the increased levels of arterial pressure persist for several days after the cessation of the hypoxic protocol (Zoccal *et al.* 2009*a*). These findings suggest that the cellular and neurochemical mechanisms recruited by SH and CIH are different. Therefore, the neural mechanisms involved with the changes in the coupling between expiratory and sympathetic brainstem neurones, in different protocols of hypoxia, must be carefully evaluated. In our view only a fine evaluation of these sympathetic and respiratory complex neuronal networks will allow us to understand the development of cardiorespiratory dysfunctions observed in pathological conditions associated with long-term exposure to hypoxia, such as mountain sickness, chronic obstructive pulmonary disease, heart failure and sleep apnoea.

References

Aaron EA & Powell FL (1993). Effect of chronic hypoxia on hypoxic ventilatory response in awake rats. *J Appl Physiol* **74**, 1635–1640.

Abdala AP, Rybak IA, Smith JC & Paton JF (2009). Abdominal expiratory activity in the rat brainstem–spinal cord *in situ*: patterns, origins and implications for respiratory rhythm generation. *J Physiol* **587**, 3539–3559.

Ainslie PN & Ogoh S (2010). Regulation of cerebral blood flow in mammals during chronic hypoxia: a matter of balance. *Exp Physiol* **95**, 251–262.

Baekey DM, Dick TE & Paton JF (2008). Pontomedullary transection attenuates central respiratory modulation of sympathetic discharge, heart rate and the baroreceptor reflex in the *in situ* rat preparation. *Exp Physiol* **93**, 803–816.

Barros RCH, Bonagamba LGH, Okamoto-Canesin R, de Oliveira M, Branco LGS & Machado BH (2002). Cardiovascular responses to chemoreflex activation with potassium cyanide or hypoxic hypoxia in awake rats. *Auton Neurosci* **97**, 110–115.

Ben-Tal A, Shamailov SS & Paton JF (2012). Evaluating the physiological significance of respiratory sinus arrhythmia: looking beyond ventilation-perfusion efficiency. *J Physiol* **590**, 1989–2008.

Bernardi L, Porta C, Gabutti A, Spicuzza L & Sleight P (2001). Modulatory effects of respiration. *Auton Neurosci* **90**, 47–56.

Bochorishvili G, Stornetta RL, Coates MB & Guyenet PG (2012). Pre-Bötzinger complex receives glutamatergic innervation from galaninergic and other retrotrapezoid nucleus neurons. *J Comp Neurol* **520**, 1047–1061.

Braga VA, Soriano RN, Braccialli AL, de Paula PM, Bonagamba LG, Paton JF & Machado BH (2007). Involvement of L–glutamate and ATP in the neurotransmission of the sympathoexcitatory component of the chemoreflex in the commissural nucleus tractus solitarii of awake rats and in the working heart–brainstem preparation. *J Physiol* **581**, 1129–1145.

Calbet JA (2003). Chronic hypoxia increases blood pressure and noradrenaline spillover in healthy humans. *J Physiol* **551**, 379–386.

Cerutti C, Gustin MP, Paultre CZ, Lo M, Julien C, Vincent M & Sassard J (1991). Autonomic nervous system and cardiovascular variability in rats: a spectral analysis approach. *Am J Physiol Heart Circ Physiol* **261**, H1292–H1299.

Costa-Silva JH, Zoccal DB & Machado BH (2010). Glutamatergic antagonism in the NTS decreases post-inspiratory drive and changes phrenic and sympathetic coupling during chemoreflex activation. *J Neurophysiol* **103**, 2095–2106.

Dick TE, Hsieh YH, Morrison S, Coles SK & Prabhakar N (2004). Entrainment pattern between sympathetic and phrenic nerve activities in the Sprague-Dawley rat: hypoxia-evoked sympathetic activity during expiration. *Am J Physiol Regul Integr Comp Physiol* **286**, R1121–R1128.

Ezure K, Tanaka I & Saito Y (2003). Brainstem and spinal projections of augmenting expiratory neurons in the rat. *Neurosci Res* **45**, 41–51.

Fletcher EC (2001). Physiological and genomic consequences of intermittent hypoxia: Invited review: Physiological consequences of intermittent hypoxia: systemic blood pressure. *J Appl Physiol* **90**, 1600–1605.

Forster HV, Dempsey JA, Birnbaum ML, Reddan WG, Thoden J, Grover RF & Rankin J (1971). Effect of chronic exposure to hypoxia on ventilatory response to CO_2 and hypoxia. *J Appl Physiol* **31**, 586–592.

Gilbey MP (2007). Sympathetic rhythms and nervous integration. *Clin Exp Pharmacol Physiol* **34**, 356–361.

Gilmartin GS, Tamisier R, Curley M & Weiss JW (2008). Ventilatory, hemodynamic, sympathetic nervous system, and vascular reactivity changes after recurrent nocturnal sustained hypoxia in humans. *Am J Physiol Heart Circ Physiol* **295**, H778–H785.

Guyenet PG, Darnall RA & Riley TA (1990). Rostral ventrolateral medulla and sympathorespiratory integration in rats. *Am J Physiol Regul Integr Comp Physiol* **259**, R1063–R1074.

Hainsworth R & Drinkhill MJ (2007). Cardiovascular adjustments for life at high altitude. *Respir Physiol Neurobiol* **158**, 204–211.

Hansen J & Sander M (2003). Sympathetic neural overactivity in healthy humans after prolonged exposure to hypobaric hypoxia. *J Physiol* **546**, 921–929.

Haselton JR & Guyenet PG (1989). Central respiratory modulation of medullary sympathoexcitatory neurons in rat. *Am J Physiol Regul Integr Comp Physiol* **256**, R739–R750.

Jacono FJ, Peng YJ, Kumar GK & Prabhakar NR (2005). Modulation of the hypoxic sensory response of the carotid body by 5–hydroxytryptamine: role of the 5-HT_2 receptor. *Respir Physiol Neurobiol* **145**, 135–142.

Janczewski WA & Feldman JL (2006). Distinct rhythm generators for inspiration and expiration in the juvenile rat. *J Physiol* **570**, 407–420.

Kääb S, Miguel-Velado E, López-López JR & Pérez-García MT (2005). Down regulation of Kv3.4 channels by chronic hypoxia increases acute oxygen sensitivity in rabbit carotid body. *J Physiol* **566**, 395–408.

Koshiya N, Huangfu D & Guyenet PG (1993). Ventrolateral medulla and sympathetic chemoreflex in the rat. *Brain Res* **609**, 174–184.

Lahiri S, Roy A, Baby SM, Hoshi T, Semenza GL & Prabhakar NR (2006). Oxygen sensing in the body. *Prog Biophys Mol Biol* **91**, 249–286.

Malliani A, Pagani M, Lombardi F & Cerutti S (1991). Cardiovascular neural regulation explored in the frequency domain. *Circulation* **84**, 482–492.

Malpas SC (1998). The rhythmicity of sympathetic nerve activity. *Prog Neurobiol* **56**, 65–96.

Mandel DA & Schreihofer AM (2009). Modulation of the sympathetic response to acute hypoxia by the caudal ventrolateral medulla in rats. *J Physiol* **587**, 461–475.

Molkov YI, Abdala AP, Bacak BJ, Smith JC, Paton JF & Rybak IA (2010). Late-expiratory activity: emergence and interactions with the respiratory CpG. *J Neurophysiol* **104**, 2713–2729.

Molkov YI, Zoccal DB, Moraes DJ, Paton JF, Machado BH & Rybak IA (2011). Intermittent hypoxia-induced sensitization of central chemoreceptors contributes to sympathetic nerve activity during late expiration in rats. *J Neurophysiol* **105**, 3080–3091.

Moraes DJ, da Silva MP, Bonagamba LG, Mecawi AS, Zoccal DB, Antunes-Rodrigues J, Varanda WA & Machado BH (2013). Electrophysiological properties of rostral ventrolateral medulla presympathetic neurons modulated by the respiratory network in rats. *J Neurosci* **33**, 19223–19237.

Moraes DJ, Dias MB, Cavalcanti-Kwiatkoski R, Machado BH & Zoccal DB (2012*a*). Contribution of retrotrapezoid/parafacial respiratory region to the expiratory-sympathetic coupling in response to peripheral chemoreflex in rats. *J Neurophysiol* **108**, 882–890.

Moraes DJ, Zoccal DB & Machado BH (2012*b*). Medullary respiratory network drives sympathetic overactivity and hypertension in rats submitted to chronic intermittent hypoxia. *Hypertension* **60**, 1374–1380.

Moraes DJ, Zoccal DB & Machado BH (2012*c*). Sympathoexcitation during chemoreflex active expiration is mediated by L-glutamate in the RVLM/Bötzinger complex of rats. *J Neurophysiol* **108**, 610–623.

Pagliardini S, Janczewski WA, Tan W, Dickson CT, Deisseroth K & Feldman JL (2011). Active expiration induced by excitation of ventral medulla in adult anesthetized rats. *J Neurosci* **31**, 2895–2905.

Paton JF (1996). A working heart–brainstem preparation of the mouse. *J Neurosci Methods* **65**, 63–68.

Paton JF, Dickinson CJ & Mitchell G (2009). Harvey Cushing and the regulation of blood pressure in giraffe, rat and man: introducing 'Cushing's mechanism'. *Exp Physiol* **94**, 11–17.

Paton JF & Dutschmann M (2002). Central control of upper airway resistance regulating respiratory airflow in mammals. *J Anat* **201**, 319–323.

Paton JF & Nolan PJ (2000). Similarities in reflex control of laryngeal and cardiac vagal motor neurones. *Respir Physiol* **119**, 101–111.

Powell FL (2007). The influence of chronic hypoxia upon chemoreception. *Respir Physiol Neurobiol* **157**, 154–161.

Powell FL, Huey KA & Dwinell MR (2000). Central nervous system mechanisms of ventilatory acclimatization to hypoxia. *Respir Physiol* **121**, 223–236.

Powell FL, Milsom WK & Mitchell GS (1998). Time domains of the hypoxic ventilatory response. *Respir Physiol* **112**, 123–134.

Richter DW (1982). Generation and maintenance of the respiratory rhythm. *J Exp Biol* **100**, 93–107.

Rosin DL, Chang DA & Guyenet PG (2006). Afferent and efferent connections of the rat retrotrapezoid nucleus. *J Comp Neurol* **499**, 64–89.

Ross CA, Ruggiero DA, Park DH, Joh TH, Sved AF, Fernandez-Pardal J, Saavedra JM & Reis DJ (1984). Tonic vasomotor control by the rostral ventrolateral medulla: effect of electrical or chemical stimulation of the area containing C1 adrenaline neurons on arterial pressure, heart rate, and plasma catecholamines and vasopressin. *J Neurosci* **4**, 474–494.

Rostrup M (1998). Catecholamines, hypoxia and high altitude. *Acta Physiol Scand* **162**, 389–399.

Rybak IA, Shevtsova NA, Paton JFR, Dick TE, St-John WM, Mörschel M & Dutschmann M (2004). Modeling the ponto-medullary respiratory network. *Respir Physiol Neurobiol* **143**, 307–319.

Shen L, Li YM & Duffin J (2003). Inhibitory connections among rostral medullary expiratory neurones detected with cross-correlation in the decerebrate rat. *Pflugers Arch* **446**, 365–372.

Simms AE, Paton JF, Pickering AE & Allen AM (2009). Amplified respiratory-sympathetic coupling in the spontaneously hypertensive rat: does it contribute to hypertension? *J Physiol* **587**, 597–610.

Smith JC, Abdala AP, Koizumi H, Rybak IA & Paton JF (2007). Spatial and functional architecture of the mammalian brain stem respiratory network: a hierarchy of three oscillatory mechanisms. *J Neurophysiol* **98**, 3370–3387.

Smith JC, Ellenberger HH, Ballanyi K, Richter DW & Feldman JL (1991). Pre-Bötzinger complex: a brainstem region that may generate respiratory rhythm in mammals. *Science* **254**, 726–729.

St-John WM & Paton JF (2003). Defining eupnea. *Respir Physiol Neurobiol* **139**, 97–103.

Sun QJ, Minson J, Llewellyn-Smith IJ, Arnolda L, Chalmers J & Pilowsky P (1997). Bötzinger neurons project towards bulbospinal neurons in the rostral ventrolateral medulla of the rat. *J Comp Neurol* **388**, 23–31.

Takakura AC, Moreira TS, Colombari E, West GH, Stornetta RL & Guyenet PG (2006). Peripheral chemoreceptor inputs to retrotrapezoid nucleus (RTN) CO_2-sensitive neurons in rats. *J Physiol* **572**, 503–523.

Tamisier R, Hunt BE, Gilmartin GS, Curley M, Anand A & Weiss JW (2007). Hemodynamics and muscle sympathetic nerve activity after 8 h of sustained hypoxia in healthy humans. *Am J Physiol Heart Circ Physiol* **293**, H3027–H3035.

Teppema LJ & Dahan A (2010). The ventilatory response to hypoxia in mammals: mechanisms, measurement, and analysis. *Physiol Rev* **90**, 675–754.

Zhang W, Carreno FR, Cunningham JT & Mifflin SW (2009). Chronic sustained hypoxia enhances both evoked EPSCs and norepinephrine inhibition of glutamatergic afferent inputs in the nucleus of the solitary tract. *J Neurosci* **29**, 3093–3102.

Zoccal DB, Bonagamba LG, Paton JF & Machado BH (2009*a*). Sympathetic-mediated hypertension of awake juvenile rats submitted to chronic intermittent hypoxia is not linked to baroreflex dysfunction. *Exp Physiol* **94**, 972–983.

Zoccal DB, Paton JF & Machado BH (2009*b*). Do changes in the coupling between respiratory and sympathetic activities contribute to neurogenic hypertension? *Clin Exp Pharmacol Physiol* **36**, 1188–1196.

Zoccal DB, Simms AE, Bonagamba LG, Braga VA, Pickering AE, Paton JF & Machado BH (2008). Increased sympathetic outflow in juvenile rats submitted to chronic intermittent hypoxia correlates with enhanced expiratory activity. *J Physiol* **586**, 3253–3265.

Additional information

Competing interests

The authors declare no competing financial interests.

Author contributions

K.M.C., J.H.C.-S., D.J.A.M. and D.B.Z. contributed to experiments involving nerve recordings. D.J.A.M. contributed to experiments involving neuronal and subglottal pressure recordings. L.G.H.B., D.J.A.M. and D.B.Z. contributed to experiments with conscious rats. B.H.M., D.B.Z. and D.J.A.M. contributed to the conception and experimental design, data analyses and interpretation of the findings and the preparation of this manuscript. All authors approved the final version of this manuscript.

Funding

This work was supported by São Paulo Research Foundation (FAPESP; grant nos 2006/51159-6 and 2009/50113-0), Conselho Nacional de Desenvolvimento Científico e Tecnológico (CNPQ;

grant nos 502098/2008-2 and 301147/2008-6) and FAPESP fellowship to D.J.A.M. (grant no. 2011/24050-1).

Authors' present addresses

K. M. Costa: International Max Planck Research School for Neural Circuits, Max Planck Institute for Brain Research, Frankfurt am Main, Germany.

J. H. Costa-Silva: Department of Physical Education and Sport Sciences, Federal University of Pernambuco, Vitória de Santo Antão, Brazil.

D. B. Zoccal: Department of Physiology and Pathology, Dentistry School of Araraquara, State University of São Paulo (UNESP), Araraquara, Brazil.